

DOE/NASA/50162-3
NASA TM-102476

NASA
IN-27
264343
578

The Experimental Evaluation and Application of High-Temperature Solid Lubricants

Christopher DellaCorte
National Aeronautics and Space Administration
Lewis Research Center

January 1990

Prepared for
U.S. DEPARTMENT OF ENERGY
Conservation and Renewable Energy
Office of Vehicle and Engine R&D

(NASA-TM-102476) THE EXPERIMENTAL
EVALUATION AND APPLICATION OF
HIGH-TEMPERATURE SOLID LUBRICANTS Ph.D.
Thesis - Case Western Reserve Univ., 1989
Final Report (NASA) 57 p

N90-16944

CSCL 11C G3/27

Unclass
0264343

DISCLAIMER

This report was prepared as an account of work sponsored by an agency of the United States Government. Neither the United States Government nor any agency thereof, nor any of their employees, makes any warranty, express or implied, or assumes any legal liability or responsibility for the accuracy, completeness, or usefulness of any information, apparatus, product, or process disclosed, or represents that its use would not infringe privately owned rights. Reference herein to any specific commercial product, process, or service by trade name, trademark, manufacturer, or otherwise, does not necessarily constitute or imply its endorsement, recommendation, or favoring by the United States Government or any agency thereof. The views and opinions of authors expressed herein do not necessarily state or reflect those of the United States Government or any agency thereof.

Printed in the United States of America

Available from

National Technical Information Service
U.S. Department of Commerce
5285 Port Royal Road
Springfield, VA 22161

NTIS price codes¹

Printed copy:

Microfiche copy: A01

¹Codes are used for pricing all publications. The code is determined by the number of pages in the publication. Information pertaining to the pricing codes can be found in the current issues of the following publications, which are generally available in most libraries: *Energy Research Abstracts (ERA)*; *Government Reports Announcements and Index (GRA and I)*; *Scientific and Technical Abstract Reports (STAR)*; and publication, NTIS-PR-360 available from NTIS at the above address.

The Experimental Evaluation and Application of High-Temperature Solid Lubricants

Christopher DellaCorte
National Aeronautics and Space Administration
Lewis Research Center
Cleveland, Ohio 44135

January 1990

Work performed for
U.S. DEPARTMENT OF ENERGY
Conservation and Renewable Energy
Office of Vehicle and Engine R&D
Washington, D.C. 20545
Under Interagency Agreement DE-AI01-85CE50162

CONTENTS

	Page
CHAPTER I INTRODUCTION	1
CHAPTER II Part 1: LUBRICANT DEVELOPMENT	2
CHAPTER III MATERIALS: PS200	4
CHAPTER IV APPARATUS And PROCEDURES	6
CHAPTER V RESULTS AND DISCUSSIONS	8
CHAPTER VI CONCLUSIONS: PS200	13
CHAPTER VII Part 2: LUBRICANT APPLICATION	14
CHAPTER VIII Materials: SEAL APPLICATION	15
CHAPTER IV APPARATUS AND PROCEDURES	17
CHAPTER X RESULTS AND DISCUSSIONS	18
CHAPTER XI CONCLUSIONS: SEAL APPLICATION	24
CHAPTER XII REFERENCES	26
APPENDIXES	28
TABLES AND FIGURES	33

THE EXPERIMENTAL EVALUATION AND APPLICATION OF HIGH-TEMPERATURE SOLID LUBRICANTS

Christopher DellaCorte
National Aeronautics and Space Administration
Lewis Research Center
Cleveland, Ohio 44135

SUMMARY

This dissertation describes a research program meant to develop an understanding of high-temperature solid lubrication and experimental techniques through the development of a composite lubricant coating system. This knowledge gained through this research was then applied to a specific engineering challenge, the tribology of a sliding seal for hypersonic flight vehicles.

The solid lubricant coating is a chromium carbide based composite combined with silver, which acts as a low temperature lubricant, and barium fluoride/calcium fluoride eutectic, which acts as a high-temperature lubricant. This composite coating provides good wear resistance and low friction for sliding contacts from room temperature to over 900 °C in reducing or oxidative environments. The specific research on this coating included a composition screening using a foil gas bearing test rig and the use of thin silver films to reduce initial wear using a pin-on-disk test rig. The chemical stability of the materials used was also addressed. This research indicated that soft metallic films and materials which become soft at elevated temperatures are potentially good lubricants.

The general results from the experiments with the model solid lubricant coating were then applied to a sliding seal design concept. This seal design requires that a braided ceramic fabric slide against a variety of metal counterface materials at temperatures from 25 to 850 °C in an oxidative environment. A pin-on-disk tribometer was used to evaluate the tribological properties of these materials and to develop lubrication techniques. The results of this work indicate that these seal materials must be lubricated to prevent wear and reduce friction. Thin films of silver, gold and calcium fluoride provided lubrication to the sliding materials. The data obtained and the lubrication techniques developed in this study provide important information to designers of sliding seals.

CHAPTER I

INTRODUCTION

The objective of this dissertation is to develop an understanding of high-temperature lubrication and experimental techniques through the development of a composite solid lubricant coating system. By studying the function of high-temperature lubricant materials and applicable experimental testing techniques, a knowledge base is generated which is then applied to a specific engineering challenge, the tribology of a sliding high-temperature seal for hypersonic vehicles.

Therefore, the organization of this dissertation is as follows. The first part of the thesis concentrates on the further development of PS200, a plasma-sprayed composite lubricant coating system. PS200 serves as a model material system from which the major concepts of high-temperature lubrication can be learned. The research encompasses a composition screening using a prototype foil gas bearing rig and the use of thin silver films to reduce wear. The results of this work, namely the use of specific high-temperature lubricants and the experimental techniques employed, are general in nature and can be applied to other high-temperature tribological applications. In the second part of this thesis, the concepts of high-temperature lubrication are applied to the tribological challenges of a high-temperature seal for hypersonic vehicles.

The hypersonic vehicle seal is a unique application which requires that a linear seal in sliding contact prevent leaking of hot gases from a high pressure region to lower pressure areas. To accomplish this goal, high-temperature materials must rub upon one another under chemically and mechanically aggressive conditions. In this part of the thesis, novel lubricant materials and suitable testing techniques which have been developed in part one of this thesis are employed to evaluate the feasibility of having a sliding seal in a high-temperature hypersonic vehicle environment. The results of this work provide a data base with which to make recommendations to the seal designers.

Thus, this dissertation encompasses both the general study of high-temperature lubrication and the specific application of this knowledge to a lubrication challenge which, due to recent interest in hypersonic flight, namely the National Aerospace Plane (NASP), has national importance.

CHAPTER II

Part 1: COMPOSITE LUBRICANT DEVELOPMENT, PS200

Solid lubricants are the materials of choice for lubrication problems where temperatures can reach 1000 °C (ref. 1). Traditionally, solid lubricants consist of thin films of graphite, molybdenum disulphide or Teflon. Even these materials, however, have maximum use temperatures of only about 400 °C. For higher temperatures, as might be encountered in a heat engine or space application, more novel materials and application techniques must be employed.

One material system that has shown promise for high-temperature lubrication of sliding contacts is a plasma sprayed coating called the PS200 system. Developed at NASA, Lewis Research Center, Cleveland, Ohio (ref. 2), the PS200 system is a three component composite coating made from a metal bonded chromium carbide, which forms a wear resistant matrix, to which silver and barium fluoride/calcium fluoride eutectic are added as solid lubricants. PS200 coatings can provide lubrication to sliding contacts from room temperature to 900 °C.

The PS200 coating system was investigated in a Master's Thesis by this author (ref. 3). In this thesis, the decision process which led to the exact material selection is described in addition to the processing and preparation

details of the coating. These aspects of the PS200 coating will, therefore, only be briefly described here.

PS200 type coatings are made by plasma spraying a composite powder mixture of metal bonded chromium carbide, silver and barium fluoride/calcium fluoride eutectic. All of these materials are relatively thermally and chemically stable in air, helium or hydrogen to at least 900 °C. This stability makes them well suited for use as high-temperature tribological materials.

The metal bonded chromium carbide is commercially available from the Metco company. It is designated Metco 430 NS. This powder is made by coating chromium carbide particles with a nickel-cobalt alloy. If plasma sprayed alone, the bonded chromium carbide forms a good wear resistant coating but displays high friction when used in a sliding contact. To offset this poor tribological property, solid lubricants, silver and barium fluoride/calcium fluoride eutectic, are added to the coating prior to plasma spraying.

Silver is considered a good low temperature lubricant because of its low shear strength even at low temperatures. At temperatures above 350 °C, however, silver loses its compressive strength and cannot support significant loads and is therefore not considered a good high-temperature lubricant. Silver is relatively stable to about 900 °C in most environments.

Barium fluoride/calcium fluoride eutectic is a good high-temperature lubricant because it undergoes a brittle to ductile transition at about 400 °C (ref. 4). Though not a particularly good low temperature lubricant ($\mu \sim 0.5$), it is not abrasive, even at room temperature. Like the other coating constituents, the fluorides are stable at elevated temperatures in both reducing and oxidizing environments. Appendix A illustrates some thermochemical calculations which can be done to verify the relative stability of the coating components in the anticipated environment.

In summary, the PS200 coating contains a chromium carbide wear resistant "base stock" with a low temperature lubricant, silver, and a high-temperature lubricant, the fluoride eutectic. The PS200 coating can provide lubrication over repeated heating cycles in a variety of environments over a wide range of temperatures.

The scope of the Master's Thesis included a detailed introduction to the PS200 system and a tribological composition screening of the three coating components using a pin-on-disk tribometer. Also, a study of the effect of atmosphere on the tribological performance of PS200 was made.

The first part of this dissertation will investigate the effect of coating composition on the tribological performance of the PS200 coating system using a prototype gas lubricated foil bearing rig. Though the foil bearing rides on a hydrodynamic film of air during steady-state operation, the PS200 coating is used on the journals to provide back-up lubrication during bearing start-up and shut-down when the hydrodynamic film has not developed. The general results of this work will be compared to the composition screening previously performed using the pin-on-disk rig.

An effort to reduce the initial run-in wear of PS200 and especially the initial wear of the counterface material, will be made by applying thin sputtered films of silver over the diamond ground PS200 coating prior to sliding. The objective of this work is to determine a range of silver overlay thicknesses which demonstrates improved tribological properties.

CHAPTER III

MATERIALS: PS200

The PS200 coatings tested in this program were prepared by plasma spraying composite powder mixtures. Depending upon the coating designation, the compositions range from 60 to 100 wt % metal-bonded chromium carbide. These coatings were previously tested in a pin-on-disk tribometer to determine the optimum composition. They are tested in this study using a prototype gas lubricated foil bearing rig.

Four different coatings are tested in the gas foil bearing rig. PS218 contains 100 wt % metal-bonded chromium carbide, PS200 contains 80 wt % metal-bonded chromium carbide and 10 wt % each of fluoride eutectic and silver. PS212 contains 70 wt % metal-bonded chromium carbide and 15 wt % each of fluoride eutectic and silver. PS213 contains 60 wt % metal-bonded chromium carbide and 20 wt % each of fluoride eutectic and silver. Other compositions which lacked one lubricant or the other were previously tested and found to be unsatisfactory and are therefore not included in the present research program (ref. 5). The exact composition and particle sizes of the components are given in table I. The coatings are applied using plasma spraying which is briefly described below.

Plasma spraying is an ideal procedure for applying materials that have varied melting temperatures onto surfaces without causing significant substrate heating. The basic plasma spray process is as follows: a stream of argon carrier gas is electrically ionized/heated between an anode and cathode to at least 10 000 K. The coating powder mixture is forced into this hot gas stream where it melts. The hot argon and melted powder mixture then impinges onto the cold (room temperature) substrate. Prior to deposition, the substrate is usually sand blasted to roughen the surface. The coating mixture "splats" and adheres to the substrate forming a strong, adherent coating. Figure 1 shows the plasma spray process schematically. The substrate is usually held in a rotating or traversing lathe chuck and the plasma spray gun is passed over the part. This process deposits approximately 0.013 mm of coating per pass. Many passes are required to build up the thick (0.37 mm) coating tested in this study. Typical plasma spray parameters are given in table II. Figure 2 is a photograph of a plasma sprayed bearing journal.

The plasma sprayed surface is a rough, tribologically poor surface. In order to achieve a good friction and wear surface the rough coating must be diamond ground. Diamond grinding also provides a convenient method of achieving a final dimension or close tolerances.

The diamond grinding procedure has been developed to obtain good, consistent wear surfaces from the plasma sprayed coatings. The general procedure is as follows: A #150 grit diamond grinding wheel is used with deionized water

lubrication to grind the coating surface. Initial rough cut grinding passes are made at a depth of no more than 0.025 mm. When the coating thickness is within 0.025 mm the grinding depth per pass is reduced to 0.010 mm. If the grind depths per pass are too large the soft phase materials, namely the silver and eutectic, will be "plucked" from the surface leaving raised carbide rich areas which act as a grinding wheel to the sliding counterfaces. If the grinding depth per pass is too small the nickel-cobalt binder material will smear over the entire surface leaving a nickel-cobalt wear surface with no lubricant exposed. Appendix B explains the grinding procedure in greater detail. Figure 3 shows a coating surface after diamond grinding. The "speckled" appearance of the coating in this figure indicates that the soft phases are present at the coating surface.

Foil Bearings

In the composition screening using the foil bearing apparatus, the journal was coated with a PS200 type coating which was then diamond ground to achieve a uniform surface finish and dimensional tolerances. The coated journals were slid against preoxidized Inconel X-750 foil bearings. The foils were heat treated after manufacture to achieve adequate spring properties needed for the successful operation of the foil bearings. The foil bearing assembly consists of a 0.1 mm thick smooth foil which is backed up or rather supported by a 0.1 mm thick corrugated bump foil. Both foils are spot welded to a keyway which is pinned to the bearing housing. Figures 4(a) and (b) give the dimensions of the bearing. Table III gives the composition of the Inconel X-750 used for the foils.

Silver Film Overlay Materials: Pin-on-disk specimens

To reduce the initial or run-in wear of the counterface materials when slid against PS200 type coatings, sputtered silver films were applied over the diamond ground surface of the disk specimens. The pure silver films were applied using a dc-magnetron sputter coater. Prior to silver deposition, the diamond ground surface was cleaned with levigated alumina and water, then rinsed in deionized water and dried. The sputter parameters were: power, 0.05 kW; argon flowrate; ~10 cc/min; chamber pressure, 50 mtorr; and target to specimen distance, ~25 mm.

The silver film thickness range from 25 to 350 nm. The thickness was determined by calibrating the sputter coater. This calibration was accomplished by sputtering for different time periods onto stainless steel coupons and using stylus surface profilometry to find the film thickness. By plotting the thickness versus time data, a calibration factor in nanometer/minute was determined for the particular parameters used. The silver film thickness on the specimens was then determined by multiplying the calibration factor by the sputtering time. For these experiments, the calibration factor is 5 nm/min.

The disk specimens which were sputtered with silver were slid against hemispherically tipped (radius = 4.76 mm) Stellite 6B pins. The composition of the pins is given in table III. The hardness is Rockwell C-42. This alloy has shown good results as a counterface material for the PS200 coatings and has been chosen as a piston ring material for a Stirling engine tested at NASA (ref. 6).

CHAPTER IV

APPARATUS AND PROCEDURES

Test Apparatus

Figure 5 is an illustration of the foil bearing test rig used in this study. A complete description of the apparatus is given in reference 7. The features important to this study are outlined below.

The test apparatus is designed to run unattended. The motor is controlled by timer switches which start and stop the motor over a 20 sec test cycle. The test specimens are heated by a quartz radiant type heater. The heater box splits in half to facilitate specimen inspection and removal. The heater is controlled by a solid state controller which measures bearing temperature with a thermocouple located on the foil bearing housing in the immediate vicinity of the test bearing. The overall duration of a set of test cycles is controlled by on/off type programable timer switches that override the cycle timer switches and the heater controller. These programmable timer switches make it possible to control the overall duration of a test as well as when the heaters are operating.

The test spindle is driven by a 1 hp electric motor and rotates at 13 800 rpm. The spindle is turned on for 13 sec and off for 7 sec giving a total cycle time of 20 sec. This cycle duration allows the test bearing to fully lift off after startup and come to a complete stop after motor shut down. A fiber optics probe is used to measure the spindle speed and count each cycle. Safety features for the test rig include oil and bearing over temperature alarms, torque overload alarm, and spindle bearing oil supply and oil return flow alarms. The test rig is shut off automatically if an alarm is tripped.

The foil bearing is mounted in a housing which, after lift off, floats over the rotating test journal on a hydrodynamic film of air. The bearing housing was loaded with deadweights to provide a 14 KPa (2 psi) static load on the bearing.

Bearing housing rotation is prevented by a torque arm that bears against a stationary cantilevered flexure plate located above the test bearing. The degree of deflection of the plate is a function of the applied torque and is measured using a capacitance probe which is calibrated at room and elevated temperatures.

The journal velocity and bearing torque were continuously recorded by a strip chart recorder. An oscillograph recorder was used to study experimental transients.

Test Procedure

The coated test journals were vacuum baked at 150 °C for 3 hr to remove any volatile residue remaining from the grinding operation and subsequent handling. The journals were then cleaned with pure ethyl alcohol, lightly scrubbed with levigated alumina, rinsed with deionized water and dried. The cleaned journal was mounted onto the test spindle and the runout was reduced

to less than 0.00750 mm by indexing the journal with respect to the spindle or using appropriate shims.

The foils were placed in the bearing housing and held in place by tapered pins driven through the foil keys. The bearing housing assembly was then mounted on the test journal, the motor started and bearing lift off verified. Figure 5 is a drawing of the assembled bearing and journal.

The tests were run in a series of six sets of 1500 start/stop cycles or a total of 9000 start/stop cycles for each test journal and foil. The tests may be terminated earlier if the torque or specimen wear become unacceptably high. Each set of 1500 cycles was run over the entire temperature range of room temperature to 650 °C degrees in the following order:

For the first 1500 cycle set the bearing was run:

- 500 start/stops at 650 °C
- 500 start/stops at 25 °C
- 500 start/stops during heating from
25 °C to 650 °C

For the following sets the bearing was run:

- 500 start/stops at 25 °C
- 500 start/stops during heating from
25 °C to 650 °C
- 500 start/stops at 650 °C

The initial set was run first at 650 °C and then at room temperature to allow the coating to run-in at the highest temperature because, initially, it may be less abrasive to the thin foil. Test sets 2 through 6 were run as outlined above to simulate the gradual heating of a bearing and to facilitate test temperature programming. The bearing temperature for the 500 start/stop cycles during the heating mode was monitored and plotted in figure 6. Figure 7 shows a typical torque versus time trace for one cycle. Foil wear and journal wear were measured at the end of each set using micrometers. A surface profile of the journal was made after testing to more accurately determine coating wear.

Sputtered Silver Films: Pin-on-disk Experiments

Apparatus. - A pin-on-disk apparatus was used in this study (fig. 8). With this apparatus, a hemispherically tipped pin was loaded against a rotating disk by means of dead weights which produced a normal load of 4.9 N. The friction force was continuously measured with a temperature compensated strain gage bridge. The pin wore a 51 mm diameter wear track on the disk and the disk wore a flat circular wear scar on the pin. Sliding was unidirectional and the velocity in these experiments was 2.7 m/sec. The disk was heated by a low frequency induction coil. Disk surface temperatures were monitored on the wear track 90° ahead of the sliding contact with an infrared pyrometer capable of measuring temperatures from 100 to 1400 °C with ±5 percent accuracy.

Procedures. - The test duration was 3 hr, 1 hr at each of the three test temperatures in the following order; 760, 350, and 25 °C. If the specimens were run first at 25 °C, then at 350 °C and then at 760 °C, the results at 25 °C would not agree with data collected during subsequent room temperature tests after the specimens had been run at elevated temperatures. This is due, in part, to diffusion of the silver overlay into the PS200 coating, the majority of which occurs during heating to the elevated test temperatures. By testing the specimens first at 760 °C then at 350 °C and finally at 25 °C, however, the data taken at 25 °C agree well with steady state values.

Rider wear was measured every 20 min by removing the pin and measuring the resulting circular wear scar on the hemispherical surface from which the wear volume was calculated. Locating dowels on the rider holder assured accurate relocation of the pin. Disk wear was measured after each hour by recording a surface profile across the disk wear track, computing the area of removed/displaced coating and multiplying by the circumference of the wear track to obtain the wear volume.

Prior to testing, the test chamber was closed and then purged for 10 min with nitrogen gas. Helium test gas was then purged for 10 min before the test was begun. The tests are conducted in a pure helium atmosphere to simulate conditions in a Stirling engine. After elevated temperature tests, the specimens were cooled to below 150 °C before opening the test chamber to inhibit specimen oxidation which might have invalidated later analysis.

CHAPTER V

RESULTS AND DISCUSSION

Foil Bearing

Torque. - The torque data has been published in reference 8 and is summarized in table IV. The uncertainties reported represent the standard deviations of the test data from repeated experiments. The significant amount of data overlap indicate that, under these conditions, the coating composition does not have a large effect on the starting or stopping torque of the test bearing. The general use of reporting uncertainties is explained in appendix C.

The starting torque over the entire temperature range was lower than the stopping torque. This can be attributed, in part, to the friction in the torque measuring assembly which reduces the measured starting torque during bearing start-up. Both the starting and stopping torque at room temperature was higher than at 650 °C. This is probably due to the increased lubrication effect of the eutectic and metal oxides present at the sliding interface during elevated temperature tests.

Foil Wear

The foil wear data is given in table V. Foils that were run against the unmodified coating, PS218, showed severe wear. In fact, these tests had to be

prematurely ended after 3000 start/stop cycles because foil wear had exceeded 33 percent of the original foil thickness, the predetermined failure point. One test with the PS218 coating was continued to confirm that the high wear rate was a steady state condition and not the result of run-in type wear. The foil bearing specimen from this test was severely worn, exhibiting a 55 percent reduction in the original foil thickness after 9000 start/stop cycles.

Markedly lower wear occurred for foils sliding against the modified coatings PS200, PS212 and PS213 than for foils sliding against the unmodified coating, PS218. The use of PS212 (70 wt % metal bonded Cr_3C_2 , 15 wt % each of silver and eutectic) resulted in the lowest foil wear, with a loss of only 17.5 percent in foil thickness after the 9000 start/stops. The use of PS200 and PS213 resulted in slightly higher foil wear which was 25 percent and 22.5 percent of the foil thickness respectively. Therefore, the PS212 coating is optimum for this coating system, in terms of minimum foil wear.

Coating Wear

Table VI summarizes the journal coating wear. The coating wear for the modified coatings follows the same trend as the foil wear. PS212 had the lowest wear factor, $6.5 \times 10^{-6} \text{ mm}^3/\text{N-m}$, followed by PS200 and PS213 which had wear factors of 8.8×10^{-6} and $10.7 \times 10^{-6} \text{ mm}^3/\text{N-m}$ respectively. The unmodified coating, PS218, exhibited, by far the lowest coating wear factor, $1.7 \times 10^{-6} \text{ mm}^3/\text{N-m}$. This result, however, is inconsequential when the unacceptable foil wear is taken into account. Appendix D explains the wear factor and how it relates to these tests.

Discussion of Test Results

All three of the modified coatings, PS212, PS200 and PS213, successfully completed the 9000 start/stop test sequence. The unmodified coating showed the lowest coating wear but displayed unacceptably high foil wear which caused test termination at only 3000 start/stop cycles.

Among the three modified coatings, PS212 displayed the lowest coating wear and the lowest foil wear (See figs. 9 and 10). One plausible reason for this behavior can be seen by comparing the transfer films from the coating which accumulate on the foil surface during testing. Figure 11 shows the EDS x-ray (Energy Dispersive x-ray Spectroscopy) level spectra of the foil surfaces after sliding against the modified coatings. The foil slid against PS212 had the highest levels of silver and eutectic (indicated by Ca and Ag peaks on fig. 17(b)) at the sliding surface.

Since lubricant transfer has been determined in a previous study (ref. 5) as beneficial to low friction and wear with this coating system, this may be a reason why PS212 performed better than the other modified coatings. The transfer materials acted as a low shear strength film at the sliding interface, reducing the wear of the coating and counterface foil material.

Figure 12 is the EDS x-ray spectrum of a foil surface after sliding against the unmodified coating, PS218. No elements were detected except those present in the foil material, Inconel X-750. Thus, there was no transfer of

material from the coating to the foil surface. This effect is probably due to the rapid wear rate of the foil; any material transfer to the foil from the coating was quickly worn away by the journal. When sliding against Inconel X-750 foils, the unmodified coating acts as an abrasive counterface material unlike the modified coatings which seem to act as reservoirs of the foil bearing lubricants.

Comparison to Pin-on-disk Results

The results of the foil bearing optimization were similar to the optimization results obtained previously using a pin-on-disk tribometer. The ranking of the wear data was the same, with PS212 outperforming the other modified coatings in terms of coating and counterface wear. PS218, however, displayed the lowest coating wear in the foil bearing tests and the highest wear in the pin-on-disk studies. This is probably due to the differences in the contact pressures/load used in the two test configurations.

The foil bearing rub tests were conducted under a 14 kPa (2 psi) load. The pin-on-disk screening test had a nominal contact pressure of 700 kPa (100 psi) after initial run in of the pin tip had occurred. This large difference in contact stress probably caused the difference in coating wear behavior. Also, because of this markedly different load, it was expected that the friction results might also differ.

In general, the friction force under light loads can usually be attributed to adhesion effects, while at higher loads shearing of a lubricating surface film becomes a predominant factor. Since the foil bearings operate under light loads, the friction force is dominated by the adhesion of the foil material to the journal and the shear properties of the surface films had little effect on the friction. The pin-on-disk tests, however, were run under higher loads and, here, the shearing of the surface films significantly affected the friction. Thus, for the foil bearings the surface film composition had little effect on the friction and hence it was approximately the same for all the specimens. In contrast, the friction in the pin-on-disk tests was affected by the coating composition.

It would be illuminating to run tests using both rigs at the same loads and speeds. However, this is not possible due to physical limitations of the equipment. The foil bearing cannot support a radial load of more than 70 kPa (10 psi), only 10 percent of the load capability of the pin-on-disk rig. In addition, due to the friction in the loading mechanism, the pin-on-disk rig is not accurate at the low loads tested in the foil bearing rig.

Clearly, because of the significant differences in the test conditions between the two test rigs it is difficult to make direct comparisons of the data. However, PS212 showed the best results for both testers. Since the foil bearing tests represent actual turbine bearings, the superior performance of PS212 under both conditions suggests that the pin-on-disk test configuration is a good screening tool for ranking friction and wear properties.

Bearing Load Capacity

The load capacity of foil bearings is an important bearing parameter which is dependent, in part, upon the geometry of the bearing and upon the gas lubricating film that develops between the rotating shaft and the foil. Since the gas lubricating film is thin, typically less than $2.5\text{ }\mu\text{m}$, the surface topography of the journal, particularly surface roughness, can have a significant effect on the fluid flow in the gas film and, hence, on the load capacity as well.

Therefore, the load capacity of the bearing was ascertained for the following three journal surfaces: a fully dense, polished Inconel 718 journal, an "as ground" plasma-sprayed PS200 coating and a plasma-sprayed PS200 coating that had been run-in over 1000 start/stop cycles. The surface finishes of the test specimens were $0.101\pm 0.005\text{ }\mu\text{m}$ for the stainless steel journal, $0.81\pm 0.05\text{ }\mu\text{m}$ for the "as ground" PS200 journal and $0.152\pm 0.010\text{ }\mu\text{m}$ for the run-in PS200 journal.

The procedure for determining the load capacity was as follows: The journal is started and the bearing was allowed to completely lift off at the customary 14 KPa (2 psi) load and a shaft surface velocity of 26.7 m/sec after lift-off. Deadweights were added to the bearing housing at 100 g (1.4 KPa) increments and the bearing was allowed to stabilize at the new load. A torque reading was recorded. The load was increased until the torque rose sharply and the bearing temperature increased indicating sliding contact. This procedure was repeated two more times to achieve confidence in the load capacity measurement.

The results of the load capacity tests are given in table VII and plotted in figure 13. The Inconel 718 journal had the highest load capacity, 51 KPa (7.3 psi) followed by the run-in plasma-sprayed coating, 41 KPa (5.9 psi). As expected, the rough as ground plasma-sprayed surface had the lowest load capacity, 28 KPa (4 psi). It should be understood that these are the load capacities at 26.7 m/sec. Surface velocities are much higher for foil bearings in turbomachinery, and the load capacity would be correspondingly much higher. However, the relative ranking of the three types of journal surfaces are expected to be the same at these higher velocities.

The trend of load capacity versus surface finish indicates that the plasma-sprayed coatings cannot support maximum loads during initial operation but can support much higher loads after a brief run-in period that smooths out the coating surface.

Much theoretical work has been done to try to explain the effects of surface roughness on the load capacity of gas bearings (ref. 9). The results of this work show the same general trends as the data presented here, but the theoretical relationships in the literature are not consistent with one another.

In general, the load capacity increases with surface roughness when the direction or lay of the roughness or wear pattern is perpendicular or transverse to the flow direction and decreases if the roughness direction is parallel or longitudinal to the flow direction. Longitudinal roughness occurs on a journal during o.d. grinding and from the wear process itself. Transverse wear seldom occurs naturally.

When the wear is longitudinal, the wear grooves or valleys provide a path for the load bearing fluid film to leave the high pressure zone, lowering the load capacity of the film. On the other hand, if the grooves are perpendicular to the flow direction they serve to help "pump" more fluid into the film, increasing the pressure and the load capacity. These effects are true only when the bearing width is much greater than the film thickness as is the case for these foil bearings.

Since both the grinding and the wear process produce longitudinal grooves in these foil bearings, the load capacity, as predicted by theory, varies inversely proportional to the surface roughness.

Silver Overlay Results: Pin-on-disk Experiments

The test results have been published in reference 10 and are given in table VIII. Depending on the thickness of the silver film applied to the disks, the friction coefficients ranged from 0.16 ± 0.02 to 0.34 ± 0.04 at room temperature, 0.16 ± 0.02 to 0.28 ± 0.03 at 350°C , and 0.20 ± 0.03 to 0.40 ± 0.04 at 760°C . Wear factors ranged from $3.0 \pm 1.5 \times 10^{-8}$ to $1.1 \pm 0.2 \times 10^{-6} \text{ mm}^3/\text{N-m}$ for the pin and $1.0 \pm 0.3 \times 10^{-6}$ to $2.2 \pm 0.4 \times 10^{-5} \text{ mm}^3/\text{N-m}$ for the coating.

The tribological performance of the PS200 coating without a silver overlay, the control case, was good and agrees well with previous data. Friction coefficients were between 0.19 ± 0.02 and 0.26 ± 0.03 and average wear factors were reasonably low. When a 100 nm thick silver overlay was applied to the PS200 coating the test results were significantly improved. Friction coefficients were between 0.16 and 0.20 and total wear of the pin, after 3 hr of testing, was reduced by a factor of three.

Discussion of Experimental Results

The initial purpose of this program was to reduce the run-in wear of counterface materials when slid against the PS200 coating. By achieving this goal, the overall life of a device or an application can be greatly increased.

Figure 14 is a plot of pin wear volume versus sliding distance for both the control case and the PS200 coating with a 100 nm thick silver film overlay. Though the graph incorporates data from three different test temperatures, the curve is relatively smooth. The data indicate that the total pin wear after 3 hr of sliding was about three times greater for the control case than for the pin slid against the PS200 coating with a 100 nm thick silver overlay film. Considering experimental error, the slopes of the curves, after run-in wear ends ($0.12 \pm 0.01 \times 10^{-2} \text{ mm}^3/\text{min}$ for the control coating and $0.10 \pm 0.01 \times 10^{-2} \text{ mm}^3/\text{min}$ for the 100 nm silver overlay case), are approximately the same after 100 min of sliding. Thus, the silver film did not significantly affect the steady state wear properties of the PS200 coating. Rather, the data suggests that the difference in total pin wear was due to the reduction in the run-in wear by the use of the silver overlay. Similar results were obtained for film thicknesses of 75, 125 and 150 nm. Thinner films did not seem to significantly reduce run in wear and plowing of the silver film was observed when thicker films were tested. This plowing lead to excessive silver transfer to the pin and higher friction especially at elevated temperatures. Thus, from these preliminary tests, a silver film overlay thickness between 75 and 150 nm provided the greatest benefit.

When investigating the abrasivity of one material to another it is instructive to consider the ratio of the wear factors (i.e., the wear factor of the pin divided by the wear factor of the disk coating). The larger the ratio, the more abrasive the coating is to the pin and vice-versa.

Table IX contains the wear factor ratio tabulated with the silver film thickness and test temperature. Figures 15(a), (b) and (c) are plots of the wear factor ratio versus film thickness for the three test temperatures. When these plots are inspected, several trends become apparent.

At 25 °C the ratio is about 0.10 for the control case (with no silver overlay). As the silver film thickness is increased from 25 to 100 nm, the ratio is decreased from about 0.11 to 0.02. That is, the silver film reduced the abrasivity of the coating to the pin up to a film thickness of 100 nm. Films thicker than about 150 nm did not result in a further wear factor ratio reduction.

At 350 °C there is no clear trend in the data. This may be due, in part, to the fact that at elevated temperatures silver has low compressive strength and, by itself, is not an adequate lubricant.

At 760 °C there was no relationship between the film thickness and the ratio, but the silver films did reduce the ratio by approximately a factor of two compared to the control case. One plausible reason for this behavior is that the tests at 760 °C were the initial tests for each specimen. In these cases, the silver film merely served to smooth out and fill in the imperfections in the plasma-sprayed surface leading to reduced pin wear. But since the silver has low compressive strength at 760 °C the benefit was not a function of silver film thickness.

The application of silver films around 100 nm thick reduced the run in wear of the pin without causing plowing and excessive silver transfer to the pin surface. The silver film acted as a run-in lubricant which smoothed out the surface and reduced the initial abrasivity of the PS200 coating to the counterface material.

CHAPTER VI

CONCLUSIONS

Foil Bearings

1. PS212 is the optimum coating composition for this application. It displayed the lowest foil wear and survived over 9000 start-stop cycles. The unmodified coating, PS218, wore the foil beyond acceptable limits after only 3000 cycles.

2. The friction of the coating for this lightly loaded, conforming geometry bearing is not significantly affected by the coating composition.

3. The diamond ground, plasma-sprayed coating can support only light loads during initial operation but can support much higher loads after a brief run-in period that smooths the coating surface.

4. The addition of silver and barium fluoride/calcium fluoride eutectic to the metal bonded chromium carbide significantly reduces the counterface material wear while increasing the journal coating wear (within acceptable limits).

Sputtered Silver Films: Pin-on-Disk Experiments

1. The run-in wear of counterface materials, when slid against PS200, appears to be reduced by applying thin silver films over the as ground, plasma-sprayed surface.

2. The friction and wear of the counterface material is affected by the thickness of the silver film overlay. Films between 75 and 100 nm thick seem to improve the counterface wear properties without adversely affecting the friction coefficient or coating wear.

3. The reduction in counterface wear obtained by this method may significantly increase the overall life of a component or application.

Relevance to Seal Application

The general results from Part 1 of this dissertation can be applied in Part 2 to the seal application. The relevant general results are as follows.

1. Silver is a good low to moderate temperature lubricant when used as a thin film or as a bulk component of a composite.

2. The fluorides function well as high-temperature lubricants.

3. Laboratory test methods such as pin-on-disk can yield meaningful results especially if the test conditions such as load, speed, temperature and chemistry simulate those anticipated in the application.

CHAPTER VII

Part 2: HIGH TEMPERATURE LUBRICATION APPLICATION

The second part of this dissertation examines a unique tribological research opportunity: the development and evaluation of a lubrication method for the engine and airframe seals for hypersonic vehicles such as the proposed National Aerospace Plane (NASP). Figure 16 shows an artist's conception of a hypersonic flight vehicle. The hypersonic craft may require flexible sliding seals in parts of the engine and for moveable airframe components. These high-temperature seals are a challenge in the development of hypersonic vehicles. Figure 17 shows, schematically, a conceptual engine seal design.

The primary design concept for this seal application has been developed at NASA Lewis Research Center (ref. 11). It consists of a spring loaded ceramic rope which forms a linear seal. The ceramic rope is woven from a high-temperature alumina-boria-silicate fabric which is capable of withstanding temperatures in excess of 1200 °C. The successful operation of this seal

depends upon its ability to slide back and forth over the counterface material without breaking the ceramic rope or causing damage to the counterface. Also, to reduce seal articulation power requirements, the friction between the lightly loaded seal rope (estimated at 50 psi) and its counterface must be as low as possible.

The design requirements of the hypersonic engine also place significant restrictions on the use of seal lubricants. One restriction is that in order to maximize active cooling of the seal components, the chosen lubrication method must not thermally insulate the engine panels. This requirement can be satisfied by using materials with high thermal conductivities or very thin films. Another restriction, which precludes the use of PS200, is that the chosen lubricant must be flexible to accommodate large engine panel distortions. Because of its high ceramic content, PS200 is not flexible. Furthermore, the materials must also be chemically compatible with the candidate seal and counterface materials.

Therefore, the second part of this dissertation encompasses a test program to determine the feasibility of having a sliding seal exposed to aggressive hypersonic vehicle and engine environment and to determine baseline friction and wear properties of some of the candidate materials. Also, life prediction of the components needs to be addressed. This data is crucially needed to evaluate and possibly modify the initial seal design.

In addition to setting up a test program for this unique situation, lubrication methods and materials for the proposed seal will be developed. The goal of this phase of the work is to provide recommendations to the hypersonic seal design team and thereby further the national space effort.

CHAPTER VIII

ENGINE SEAL MATERIAL

In the pin-on-disk tests which support the hypersonics engine seal program, a stainless steel pin (Nitronic 60) was wrapped with a sample of high-temperature ceramic rope fabric and then slid against a test disk made of Inconel X-750, copper or a new intermetallic, $\text{Ti}_3\text{Al-Nb}$; three candidate engine wall materials.

The fabric is woven from Alumina-Boria-Silicate fibers. The composition of the fabric, designated AF-40, is by weight, 62 percent Al_2O_3 , 14 percent B_2O_3 and 24 percent SiO_2 . This fabric has excellent strength and flexibility to temperatures over 1000 °C (ref. 12). The fabric is made from bundles of 10 μm fibers woven in a cross-over type satin harness pattern and resembles heavy burlap. Each weave bundle contains 390 fibers. Figure 18 is a photograph of the test fabric.

Fabric Lubrication Treatment

Sputtered thin films of different solid lubricants were applied over the bare fabric surface prior to sliding. The sputtered lubricants were silver, gold and calcium fluoride. Silver and gold are potentially good low

temperature lubricants because of their low shear strength and calcium fluoride is a good high-temperature lubricant because it displays ductile behavior above about 500 °C. The fabric was sputtered clean prior to lubricant deposition. The sputtering parameters are given in table X. Boron nitride (BN) was also tested as a potential fabric lubricant. This coating was applied by spraying BN, in a methylene chloride slurry, onto the fabric then allowing the methylene chloride to evaporate. This procedure produced a relatively thick (~0.1 mm) BN coating on the fabric.

The following lubricant treated fabric specimens were prepared for use in this study:

Fabric Designation	Sputtered Lubricant Coating
AF-40	100 nm Ag
AF-40	50 nm CaF ₂
AF-40	100 nm Ag + 50 nm CaF ₂
AF-40	150 nm Au
AF-40	Sprayed BN

All three of the lubricants are thermally and chemically stable to at least 900 °C in air or hydrogen, the anticipated engine environment. At elevated temperatures, BN oxidizes in air to form boric oxide which may provide a lubricating effect (ref. 13).

Seal Counterface Material: Test Disks

The counterface materials tested in this study were Inconel X-750, high purity copper (>99.9 percent pure) and a new intermetallic, Ti₃Al-Nb. Inconel X-750 is a nickel-chromium based superalloy hardened to Rockwell C-40. The surface finish of the Inconel and copper disk specimens was 0.08 and 0.1 µm respectively. The disks are 6.35 cm in diameter and 1.27 cm thick.

The Ti₃Al-Nb counterface disks are made by hot pressing Ti₃Al-Nb powders in a vacuum. The powders are prepared by the Plasma Rotating Electrode Process (PREP). Reference 14 gives a more detailed description of the intermetallic's properties and preparation procedure. The Ti₃Al-Nb contains 65 wt % Ti, 14 wt % Al and 21 wt % Nb. The hot pressed plate is 5.0 mm thick, 150 mm long and 50 mm wide. 50 by 50 mm squares were cut from the plate and polished with silicon carbide sandpaper to make the test disks. A 16 mm hole was cut into the center of the disk by wire electro machining methods. The disk surface was then polished to a 0.1 µm finish using aluminum oxide polishing powder. Scanning electron microscopy (SEM) and energy dispersive x-ray analysis (EDS) indicate that the prepared surface was free from contaminants and large scratches. Figure 19 is a photograph of the Ti₃Al-Nb wear disks.

Some of the intermetallic wear disks were coated with gold either by sputtering or ion plating. The deposition parameters are given in table X. Ion plating differs from sputtering in that the coating material is actually evaporated onto the substrate while the substrate is being sputter cleaned. This means that only the most adherent gold particles stay on the substrate surface.

Consequently, ion plating produces well adhered coatings (ref. 15). Since coating adherence is critical to lubrication it is hoped that the ion plated coatings will perform better than the sputtered coatings. Figure 20 shows, schematically, the ion plating process.

Diffusion Barrier Treatments

To function as lubricant coatings, the deposited films must not chemically react or change composition during use. Although no chemical reactions between gold and the candidate materials are expected, some diffusion, enhanced by the high test temperatures, may occur reducing the lubricating properties of the gold films. Therefore several diffusion barriers are also evaluated by performing furnace heat treatment tests at up to 700 °C, then examining the specimens for evidence of gross solid state diffusion.

Palladium is one diffusion barrier which was tested. Prior to sputter depositing a 100 nm thick gold film, a 50 nm palladium diffusion barrier was sputter deposited (see table I). The literature (ref. 16) indicates that at elevated temperatures, palladium will react with the titanium in the substrate disk to form a titanium palladium intermetallic, Ti_3Pd , reaction layer approximately 40 nm thick. This layer may then act as a diffusion barrier to prevent any intermixing of the gold lubricating film and the test disk constituents.

Rhodium was also tested as a potential diffusion barrier. It may function well because its high melting temperature, approximately 2000 °C, leads to low homologous temperatures during use. Thus, a rhodium layer may inhibit thermally activated or enhanced diffusion.

Test samples were prepared by sputter depositing 150 nm of rhodium onto heat treated coupons and wear disks. A 150 nm gold lubricant film was then sputter deposited over the rhodium.

Chapter IX

SEAL EXPERIMENTS

Apparatus

The same pin-on-disk apparatus which was used in the sputtered film study was used in this study to evaluate the candidate seal materials and the lubrication methods proposed. In these experiments, a metal pin is covered with the fabric to be tested and loaded against a rotating Inconel, copper or Ti_3Al-Nb disk by means of deadweights. The fabric was fastened to the pin with a wire loop clamp which rested in a machined groove in the outside diameter of the pin. See figure 21. The pin had a 2.54 cm radius and a 3.2 mm diameter flat spot on its tip.

Test Conditions

The sliding velocity for these tests was 0.27 m/sec (100 rpm). The applied load to the pin was 270 g which gives a nominal contact pressure between the fabric and the disk of about 50 psi. The test atmosphere during these

tests was air with a relative humidity of 35 percent at 25 °C. The maximum test temperature for the tests was 700 °C. Because of a loss in oxidation resistance above 700 °C, this temperature is considered the maximum use temperature for Ti₃Al-Nb. Copper severely oxidizes at 700 °C but is tested, nonetheless, for comparison. Because of its superior oxidative stability, Inconel is tested to 850 °C.

Test Procedure

Prior to each test, the polished disks were cleaned with ethyl alcohol, lightly scrubbed with levigated alumina, rinsed with deionized water and dried. The specimens were loaded into the test chamber and the test gas was allowed to purge the chamber for ten min before testing was begun.

The total test duration was 1 hr. The specimens were slid for the first 20 min at room temperature then slid during a ten min heating period to 700 °C (850 °C for the Inconel disks). They were then slid at 700 °C (850 °C for the Inconel disks) for 10 min and then slid for the final 20 min during cooling to 25 °C. Selected specimens were tested twice to ascertain tribological behavior after repeated test temperature cycles.

CHAPTER X

Results: INCONEL AND COPPER COUNTERFACES

These test results have been published in reference 17 and are given in table XI and graphed in figures 22 and 23. Generally, specimen wear was limited to fabric fiber breakage. The disk surface did not significantly wear (i.e., no wear track on disk was detected by stylus surface profilometry). Since fiber breakage, compared to a finite amount of abrasive wear, dramatically changes the overall structure of the fabric surface and results in higher leakage rates, it constitutes a catastrophic material failure which limits the useful life of the seal. Thus, a measure of a test's success is based upon the extent of fiber breakage and the friction coefficient. Quantitatively, for these experiments, if less than 40 fibers in any single fiber bundle are broken the wear is mild. If more than 40 but less than 100 are broken the wear is moderate. If more than 100 fibers in a single bundle are broken, the wear is considered severe.

The friction coefficient for the bare AF-40 fabric sliding against the polished Inconel disk was 0.42 ± 0.02 during initial testing at room temperature. Upon heating, the disk begins to oxidize and the friction increased. At 850 °C the friction coefficient was very high, 1.25 ± 0.06 . As the specimens were cooled, the friction coefficient decreased gradually to 0.6 ± 0.03 at room temperature. Subsequent heating and cooling cycles produced friction coefficients of 0.6 ± 0.03 at room temperature which increased, once again, to 1.3 ± 0.1 at 850 °C. Moderate fiber breakage occurred during these tests (see fig. 24).

The friction coefficient for the AF-40 fabric was decreased by approximately a factor of two when a solid lubricant film had been applied. Fabric

upon which 100 nm Ag and 50 nm CaF_2 had been sputtered displayed friction coefficients which ranged from 0.30 ± 0.02 , at room temperature, to 0.60 ± 0.03 at 850 °C. No fiber breakage was observed after these tests.

When gold was used as the fabric lubricant, the friction behavior was similar to the tests with silver and CaF_2 . Friction coefficients ranged from 0.30 ± 0.02 at room temperature to 0.60 ± 0.03 at 850 °C. No fiber breakage occurred when gold was used as the lubricant.

When the bare AF-40 was slid against a pure copper disk the friction coefficients ranged from 0.30 ± 0.02 at room temperature to 0.50 ± 0.03 at 700 °C. When tested in air, however, the copper disk surface severely oxidized at temperatures above 450 °C (ref. 18). The oxide film spalls and is therefore not passivating. Thus without a protective coating, copper is probably not a suitable counterface material. No fiber breakage was observed for these tests.

Boron nitride (BN) is not a good lubricant for this fabric. When slid in air the friction coefficient was 0.50 ± 0.03 at room temperature and increased to 1.4 ± 0.1 at 850 °C. The fabric was also chemically attacked by the BN at elevated temperatures and became very weak and brittle. This was probably because BN oxidizes to Boria (B_2O_3) above 800 °C which can act as a fluxing agent to the fabric (ref. 19).

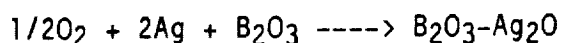
Discussion

When the AF-40, alumina-boria-silicate, fabric was slid against Inconel X-750 with no lubrication, the friction was unacceptably high. The forces arising from the high friction coefficients lead to excessive tensile stresses in the fabric fibers and ultimately fiber fracture. By sputtering lubricants onto the fabric surface the friction was reduced by providing a low shear strength film between the ceramic fabric and the metal counterface. This also lowered the tensile stresses on the fibers and fracture was less likely to occur.

At elevated temperatures, the friction coefficients were twice as high as at room temperature. One factor may be that the metal oxides which form at elevated temperatures are not very lubricious. Another contributing factor may be that the thin sputtered lubricant films tend to diffuse into the fabric away from the sliding contact upon heating. Clearly, the presence of more lubricants in the contact area may further reduce friction. To test this hypothesis a second lubrication method was investigated.

With this method, the fabric was impregnated with fine lubricant powder by placing a fabric test sample in a jar filled with Ag and CaF_2 powder. The jar was then rolled to thoroughly impregnate the fabric with lubricants. The fabric was then removed and heated in a furnace at 950 °C, just below silver's melting point, to partially sinter the lubricants in order to achieve some bonding between the lubricants and the fabric fibers. The resulting fabric was severely weakened by this treatment. In fact, the fabric could be easily broken by hand. Subsequent visual examination of the specimens indicated that a chemical reaction had occurred. This was evidenced by a molten layer present on the fabric surface even though the firing temperature was much

lower than the fabric's melting temperature. At 950 °C a reaction between boria and Ag is possible (ref. 20). It is given below:



Since this reaction weakens the fabric, this lubrication method is unsatisfactory and, hence, not recommended.

No significant fiber weakening is observed for the fabric that has been sputtered with lubricants even after a 16 hr heat treatment at 950 °C. This is probably because the thin sputtered films constitute a much smaller volume than the impregnated lubricant powders. Therefore much less of the fabric's boria content reacted. Fortunately, gold does not react with fabric yet lubricates as well as silver. Thus, gold may provide suitable fabric lubrication to 1000 °C even after following the powder lubrication method. Obtaining and efficiently using gold powder for this application method, however, would be economically and practically unfeasible. Therefore, these tests have not been done.

An SEM analysis of the fabric and the disks after testing indicates that the mode of failure for the fabric is fiber fracture. No fiber abrasion was observed. See figure 25. Energy dispersive x-ray analysis (EDS) showed that no lubricants or fibers transfer to the disk surface but there was a transfer of nickel and chromium, or copper, depending upon the test, to the fabric surface probably in the form of oxides.

Clearly, the lubrication of the fabric is necessary to prevent fiber breakage and to reduce friction to acceptable levels. The chosen lubrication method must not only provide an adequate lubricant supply to the sliding contacts for the life of the seal but must also employ lubricants which do not adversely react with the seal fabric and cause its degradation.

Results: Ti₃Al-Nb Counterface

Table XII summarizes the friction and wear data. Although the friction coefficient for the unlubricated specimens was 0.30 ± 0.03 during the initial room temperature sliding it increased further into the test. The uncertainties represent typical scatter during the tests. Generally, at least two repeat tests were performed for each material combination. At higher temperatures, the friction was higher. Figure 26 is a plot of the friction coefficients versus test temperature for a set of these specimens. At 700 °C, the friction coefficient was 1.5 ± 0.2 . Upon cooling, the friction coefficient decreased only to 1.3 ± 0.2 . Repeated test temperature cycling produced friction coefficients between 1.3 and 1.5 ± 0.2 . Severe fiber breakage (more than 100 fibers broken in a single weave bundle) occurred during these tests.

The results for the gold coated fabric sliding on the unlubricated disk are presented in figure 27. Again, the friction coefficient was low at 0.37 ± 0.03 initially at room temperature. However, upon heating, the friction increased to 1.3 ± 0.2 at 700 °C. When cooled to room temperature again, the friction decreased slightly to 1.0 ± 0.2 (fig. 27). Therefore no significant benefit was obtained by applying the sputtered gold to the fabric when slid against the intermetallic. Severe fiber breakage occurred during these tests.

When the gold sputter coated disk was slid against the bare fabric, the friction coefficient was initially low at room temperature 0.20 ± 0.03 . Like previous tests, at 700°C , the friction coefficient was high, 1.4 ± 0.2 (fig. 28). Upon cooling, the friction increased slightly to 1.8 ± 0.1 between 200 and 400°C but then decreased to 0.9 ± 0.1 at 25°C . Moderate, but unacceptable, fiber breakage (between 40 and 100 fibers broken in a single weave bundle) occurred. It was observed that the gold on the wear track of the disk was wiped off the fabric after only a few minutes of sliding which indicated poor adhesion of the sputtered film to the disk.

The friction for the disk, ion plated with the gold film, was low at room temperature, 0.20 ± 0.05 . Upon heating, the friction coefficient remained low, 0.20 , and the wear track remained gold in color until the specimens were heated to 400°C . At this temperature the friction began to increase sharply and the disk surface became dark brown in color. After 4 min of sliding above 400°C , the fabric failed completely, allowing the stainless steel pin to slide against the intermetallic disk. The tests were terminated at this point. Visual observation of the disk showed that the ion plated gold film was not longer visible even outside the wear track.

The intermetallic specimen coated with the palladium and the gold films failed the furnace heat treatment test. Although good adhesion of the films was obtained, the specimens suffered severe diffusion when heated above 400°C . After they were heated to 700°C , an x-ray photoelectron spectroscopy (XPS) depth profile was performed which indicated that the surface was primarily aluminum ($2p$ peak) with small amounts of titanium ($2p^{3/2}$ peak). These were probably in the form of oxides since oxygen was also detected (fig. 29). Neither of these oxides is a good lubricant. Therefore no tribotest specimens with palladium/gold films were tested.

The heat treatment coupons coated with rhodium and gold did not fail the static heat treatment test. At 400°C , the gold surface remained visibly yellow. After 2 hr at 700°C the surface had become violet in color but remained smooth and shiny. A post heat treatment XPS depth profile, shown in figure 30, indicates that the outermost surface layer was a thin film of rhodium ($3d^{5/2}$ peak), presumably the oxide. Under this layer was a much thicker layer of gold and titanium, aluminum and oxygen. Under this layer was a rhodium rich layer. Figure 31 shows a sketch of the layered structure following the heat treatment.

Because the near surface region contained significant gold and had a smooth surface it could provide lubrication to the fabric. Therefore, tribotest disk specimens were prepared tested.

The friction coefficient for the rhodium/gold film initially low, 0.20 ± 0.05 . The friction remained low until the test temperature reached 500°C . Then the friction increased. At 700°C , the friction coefficient was 1.0 ± 0.1 . Upon cooling to room temperature, it decreased to 0.6 ± 0.1 . The general shaped of the friction graph is similar to figure 28. After testing, the disk surface was smooth and shiny in appearance and had a violet color similar to the heat treatment sample. The fabric damage during these tests was mild (less than 40 fibers in any single bundle were broken) and is considered acceptable.

DISCUSSION

It was hoped that the bare fabric sliding against the $\text{Ti}_3\text{Al-Nb}$ intermetallic would show good tribological properties. This result, however, was not obtained. In fact, the lubrication treatments tested here, such as sputter deposited gold films, which markedly improve the properties of fabric/superalloy sliding couples studied previously (ref. 17) were not at all successful for the intermetallic disks.

The reason for this behavior, or at least a partial justification for it, can be understood by noting that the major constituent of the intermetallic is titanium. Titanium has traditionally been very difficult to lubricate, even when sliding under mild conditions such as room temperature in oils and greases (ref. 21).

The naturally occurring passivating film on titanium is a form of rutile, TiO_2 , which can prevent good bonding between lubricant films and the underlying metal. If an intermediate lubricant film is to function well, it must bond to both rubbing surfaces and be easily shearable to allow for low friction and wear. If this bonding does not occur, as is the case here, the film will not function and the surfaces will not be lubricated. This may be one reason why the intermetallic is difficult to lubricate these tests.

Another reason is that the surface of the intermetallic becomes rough when it oxidizes, which may increase the friction and wear. The surface finish of the polished disks was $0.1 \mu\text{m rms}$ and the oxide film which develops during testing or static heating had a surface finish of $0.4 \mu\text{m rms}$. Therefore, during sliding, rough oxide "asperities" may be grabbing at and breaking the individual fibers which may lead to high friction and fabric damage.

Gold was sputtered onto the fabric surface as a solid film lubricant. Since the gold does not adhere the oxide layer on the $\text{Ti}_3\text{Al-Nb}$ surface it did not transfer from the fabric to this surface and, hence, did not lubricate well. EDS analysis of the wear specimens after sliding indicted that no gold had transferred to the disk surface. Visual examination showed that most of the gold which had been sputtered onto the fabric had been worn off during sliding. Clearly, sputtering gold onto the fabric is not a good lubrication method for the sliding against the intermetallic disk.

To encourage the development of a good lubricating film, gold was next sputtered onto the polished intermetallic disk surface. By doing this, a larger volume of gold is present over the entire disk sliding area instead of only over the small pin area as was the case previously. It was hoped that by having a larger gold wear volume available, longer wear lives would be achieved. This lubrication method, however, was also unsuccessful. After only a few minutes of sliding, the pin fabric had wiped the gold off of the disk surface. This indicated that there was again a very poor bond between the gold and the substrate.

To achieve better bonding, a more energetic form of coating, ion plating was tried (ref. 22). The test results were interesting but not tribologically successful. At room temperature, the friction coefficient was very low. The gold film remained in the wear track on the disk and the friction remained low

until the specimens were heated to 400 °C. As previously stated, at 400 °C, the shiny gold film on the track turned brown and dull and the friction increased an order of magnitude.

EDS x-ray analysis of the ion plated specimen after testing, shown in figure 32, indicated that the surface had a very high concentration level of titanium and aluminum and a low concentration level of gold. When the surface was scraped with a razor blade and then re-analyzed, the gold level increased as shown in figure 33. This indicated that a surface film, probably rich in titanium dioxide, was present which covered the gold lubricating film. Since no chemical reaction between gold and the intermetallic was found in the literature, it was concluded that the gold and the intermetallic were interacting through gross diffusion at elevated temperatures. It is believed that the sputter deposited gold films did not exhibit obvious diffusion effects because the metal substrate was not sputter etched prior to gold deposition. Therefore an oxide film separated the gold from the intermetallic substrate. Although the oxide film present at the surface prevents good coating adherence, it also acts as a diffusion barrier.

Poate et al. (ref. 16) studied the interdiffusion of gold and titanium films at elevated temperatures. They found that in air, the diffusion of titanium through gold was very rapid above 400 °C. The titanium diffuses through the grain boundaries of the gold and oxidizes when it contacts the air. This oxidation process uses up free titanium at the gold/air interface creating a chemical sink for free titanium which helps to enhance the diffusion process. They estimate that the oxide layer grows to be about 40 nm thick before the process is slowed

The observation of Poate et al. (ref. 16) agrees with the results of the tribotests. At room temperature, the friction is low because the fabric is sliding on a gold film. At 400 °C, the titanium diffuses through the gold and the surface film becomes a rough, thin oxide which does not provide lubrication. Therefore, the friction increases and the fabric fails. Clearly, a diffusion barrier as well as a lubricant film is needed.

Only the ion plated gold film experienced this diffusion problem. Since the sputtering of gold onto the disk surface was done without presputter cleaning, the sputtered gold film was actually applied over an oxide layer which prevented titanium diffusion yet also prevented good adhesion.

One attempt to achieve both diffusion inhibition and lubrication was to use a palladium diffusion barrier under the sputtered or ion plated gold film. This procedure failed. Like the ion plated gold films, the specimens suffered severe diffusion when heated above 400 °C in a furnace. After a heat treatment to 700 °C, an x-ray photoelectron spectroscopy (XPS) depth profile was done which indicated that the surface was primarily aluminum oxide with some titanium oxide (fig. 29). Neither of these oxides is a good lubricant. Thus, a better diffusion barrier was needed.

One reason why the Pd film failed may be that gold and palladium can form solid solutions, especially at elevated temperatures. Thus, when the specimens were heated, the gold and palladium intermixed allowing gold and the substrate to interact. Clearly a successful diffusion barrier will be one that does not form solid solutions with either gold or the Ti₃Al substrate.

Rhodium was chosen as a diffusion barrier because its high melting temperature (~2000 °C) leads to low homologous temperatures during use which may hinder diffusional processes. Also, gold and rhodium form no solid solutions with one another even up to 1000 °C.

There was no discernible interdiffusion of the rhodium/gold films during the heat treatment tests until the temperature reached 700 °C. At 700 °C, a violet film covered the surface. The surface, however, remained smooth. After the treatment, an XPS depth profile was performed. Figure 30 shows the results. The surface layer was a thin film of rhodium (presumably the oxide) under which was thicker gold layer with significant amounts of titanium and aluminum and oxygen. Under this layer was rhodium rich layer with aluminum, titanium and oxygen (fig. 31). Although the lubricating film suffered some diffusion, because the surface region still contained significant gold and had a smooth surface finish it did provide some lubrication to the fabric.

Though the friction for the rhodium/gold film increased following the heating cycle, the fabric sustained no significant fiber breakage, probably because the smooth surface had no rough asperities to "grab" at individual fibers. This result is very encouraging because it suggests a long useful life for the seal materials. The high friction is not encouraging but can be accounted for in the final seal design (i.e., pressure balancing the seal to reduce the applied and thus reduce the actuation forces.

It is clear from these tests that the mechanical properties, such as the friction coefficient and fiber fracture, of the candidate seal materials are important. When the test temperature is high, however, the chemistry and diffusion properties of the candidate materials must also be considered.

The final recommendation to the seal designers is as follows. If $\text{Ti}_3\text{Al-Nb}$ is chosen as a counterface material it must be protected from oxidation by a diffusion barrier layer such as rhodium over which is applied a gold lubricating film. Also, after the exact seal loads, temperatures and environment is known (i.e., after a test engine has been fired), the optimization of lubricant coating techniques and thicknesses must be done to ensure the best possible tribological results.

CHAPTER XI

CONCLUSIONS: SEAL PROGRAM

1. The tribological properties of the AF-40 fabric were ascertained at temperatures from 25 to 850 °C. The friction coefficient and the extent of fiber fracture are the significant parameters upon which to measure the success of a test. Counterface disk wear was too small to measure.

2. The friction coefficient is reduced by a factor of two over the entire temperature range studied and fiber breakage is prevented by applying a thin sputtered film of silver and calcium fluoride or gold on the fabric surface prior to sliding against the Inconel disks.

3. Boron nitride does not effectively lubricate the fabric. At elevated temperatures, the boron nitride apparently oxidized to boric oxide which seemed to react with the fabric causing severe fabric degradation.

4. When present in large quantities, such as a powdered film, silver, calcium fluoride and boron nitride seem to chemically attack the fabric at elevated temperatures. This effect may be avoided by applying small quantities of the lubricants such as by using a sputtered film.

5. Gold shows promise as being a suitable solid lubricant for the AF-40 fabric. When used as a sputtered film it lowers friction by a factor of two when slid against the Inconel disks and does not react with the fabric.

6. The friction coefficient and the fabric wear for the unlubricated Ti/3/Al-Nb intermetallic disks are unacceptably high.

7. Sputtered gold films do not adhere well to the intermetallic unless the surface is sputter etched prior to gold deposition.

8. The ion plated gold films on the intermetallic disks provided effective lubrication only at room temperature. At elevated temperatures, diffusion of the substrate constituents through the gold severely reduced its lubrication effectiveness.

9. The gold films on the Ti₃Al-Nb intermetallic disks are able to provide lubrication only when a rhodium diffusion barrier is applied prior to gold deposition. The rhodium prevents gross substrate oxidation and help to maintain smooth sliding surfaces to prevent fiber breakage.

10. Successful diffusion barriers will not only prevent substrate oxidation but also prevent intermixing of the lubricant and the substrate and the lubricant and the barrier.

11. Inconel seems to be a better candidate material choice compared to copper or Ti₃Al-Nb. Friction and wear are lower and the lubrication techniques discussed work well for Inconel.

Some general conclusions can be drawn from each of the research topics described in this thesis. For instance, it is clear that when the sliding environment includes reactive gases such as oxygen and water vapor, and high-temperatures both physical and chemical properties of the materials influence the tribological properties. Also, from an engineering point of view, the friction coefficient is an intensive property. That is the coefficient itself does not define frictional losses or loads in a machine element but the applied load and the coefficient make up the important design constraints.

This concept becomes critical when designing for the starting torque for a bearing or actuation forces for an engine seal. In both of these cases the magnitude of the applied loads and the size of the component determine the forces which must be accounted for.

Tribological properties are state affected parameters. That is, the loads, speeds, contact geometry, temperatures and chemistry of an application must be known in order to accurately determine the tribological properties.

Finally, tribology is an interdisciplinary field which encompasses mechanics, physics, chemistry and materials science. In order to successfully understand tribological phenomena many aspects of a problem must be considered.

CHAPTER XII

REFERENCES

1. Ludema, K.C.; and Ajayi, O.O.: Wear Mechanisms in Ceramic Materials - Engine Applications. Proceedings of the 22nd Automotive Technology Development Contractors Coordination Meeting, SAE P-155, 1985, pp. 337-341.
2. Sliney, H.E.: The Use of Silver in Self-Lubricating Coatings for Extreme Temperatures. ASLE Trans., vol. 29, no. 3, July 1986, pp. 370-376.
3. DellaCorte, C.: Experimental Evaluation of Chromium-Carbide-Based Solid Lubricant Coatings for Use to 760 °C. NASA CR-180808, Case Western Reserve University, Masters Thesis, 1987.
4. Deadmore, D.L.; and Sliney, H.E.: Hardness of CaF_2 and BaF_2 Solid Lubricants at 25 to 670 °C. NASA TM-88979, 1987.
5. DellaCorte, C.; and Sliney, H.E.: Composition Optimization of Self-Lubricating Chromium-Carbide-Based Composite Coatings for Use to 760 °C. ASLE Trans., vol. 30, no. 1, Jan. 1987, pp. 77-83.
6. Sliney, H.E.: A New Chromium Carbide-Based Tribological Coating for Use to 900 °C with Particular Reference to the Stirling Engine. J. Vac. Sci. Technol. A, vol. 4, no. 6, Nov.-Dec. 1986, pp. 2629-2632.
7. Wagner, R.C.; and Sliney, H.E.: Effects of Silver and Group II Fluorides Addition to Plasma-Sprayed Chromium Carbide High Temperature Solid Lubricant Coatings for Foil Gas Bearings to 650 °C. NASA TM-86895, 1984.
8. DellaCorte, C.: Tribological Composition Optimization of Chromium-Carbide-Based Solid Lubricant Coatings for Foil Gas-Bearings at Temperatures to 650 °C. Surf. Coatings Technol., vol. 36, no. 1, 1988, pp. 87-98 (NASA CR-179049).
9. Sun, D.C.: On the Effects of Two-Dimensional Reynolds Roughness in Hydrodynamic Lubrication. Proc. R. Soc. Lond. A., vol. 364, no. 1716, Dec. 12, 1978, pp. 89-106.
10. DellaCorte, C.; Sliney, H.E.; and Deadmore, D.L.: Sputtered Silver Films to Improve Chromium Carbide Based Solid Lubricant Coatings for Use to 900 °C. STLE Tribology Trans., vol. 31, no. 3, July 1988, pp. 329-334 (NASA TM-100783).

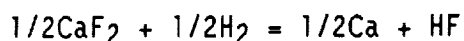
11. Steinetz, B.M.; DellaCorte, C.; and Sirocky, P.J.: On the Development of Hypersonic Engine Seals. NASA TP-2854, 1988.
12. Sawko, P.M.; and Tran, H.K.: Strength and Flexibility Properties of Advanced Ceramics Fibers. SAMPE Q., vol. 17, no. 1, Oct. 1985, pp. 7-13.
13. Bowden, F.P.; and Tabor, D.: The Friction and Lubrication of Solids, Part II. Clarendon Press, Oxford, 1964, pp. 206-209.
14. Brindley, P.K.: SiC Reinforced Aluminide Composites. High Temperature Ordered Intermetallic Alloys II, N.S. Stoloff, et al., eds., MRS Symp. Proc. Vol. 81, Materials Research Society, Pittsburgh, PA, 1987, pp. 419-426 (NASA TM-100956).
15. Spalvins, T.; and Buzek, B.: Frictional and Morphological Characteristics of Ion-Plated Soft Metallic Films. Thin Solid Films, vol. 84, 1981, pp. 267-272.
16. Poate, J.M.; Tu, K.N.; and Mayer, J.W.: Thin Films - Interdiffusion and Reactions. Wiley, 1978, pp. 341-355.
17. DellaCorte, C.: Tribological Properties of Alumina-Boria-Silicate Fabric from 25 °C to 850 °C. STLE Tribology Trans., vol. 32, no. 3, July 1989, pp. 325-330 (NASA TM-100806).
18. Lustman, B.: Resistance of Metals to Oxidation at Elevated Temperatures. Metals Handbook, T. Lyman, ed., American Society for Metals, 1948, pp. 223-227.
19. Deacon, R.F.; and Goodman, J.F.: Lubrication by Lamellar Solids. Proc. R. Soc. London, A., vol. 243, no. 1235, Feb. 11, 1958, pp. 464-482.
20. Levin, E.M.; and McMurdie, H.F., eds.: Phase Diagrams for Ceramists, 1975 Supplement. Figure 4261, American Ceramic Society, 1975, p. 79.
21. Braithwaite, E.R.: Solid Lubricants and Surfaces. The MacMillan Co., New York, 1964, p. 229.
22. Miyoshi, K.; Spalvins, T.; and Buckley, D.H.: Tribological Characteristics of Gold Films Deposited on Metals by Ion-Plating and Vapor Deposition. 3rd International Conference on Solid Lubrication, ASLE SP-14, ASLE, Park Ridge, IL, 1984, pp. 208-216 (Also, Wear, vol. 108, 1986, pp. 169-184).

APPENDIX A

THERMOCHEMICAL CALCULATIONS

The calculation of chemical reactivities between potential lubricant materials and expected operating environments is illustrated in this appendix. Equilibrium constants for presumed reactions are calculated at several temperatures to determine the relative stability of the proposed lubricant material. Small product partial pressures (less than 10^{-4}) indicate that the material is stable under the environmental conditions being considered. The following are calculations of the chemical reactivity between CaF_2 and hydrogen at 760°C .

The presumed reaction is as follows:



hence, the expression for the equilibrium constant is:

$$K_{\text{hydrogen}} = P_{\text{HF}} / (P_{\text{hydrogen}})^{1/2}$$

where P_{HF} and P_{hydrogen} represent the partial pressures of the hydrogen-fluoride and hydrogen gas respectively. A hydrogen partial pressure of one atmosphere is assumed for these calculations.

The pressure of the hydrogen-fluorine gas is used to determine the relative reactivity of the CaF_2 . By using tabulated values for the equilibrium constant, K , it is seen that the hydrogen-fluorine partial pressure is insignificant under these conditions:

$$K_{\text{hydrogen}} = 1.0 \times 10^{-13} \text{ at } 760^\circ\text{C}.$$

$$P_{\text{HF}} = 10^{-13} \text{ atm}$$

No significant reaction. Therefore CaF_2 is stable in hydrogen at 760°C . A similar calculation for CaF_2 in oxygen yields $P_{\text{HF}} = 10^{-27}$; no significant reactivity. Thus CaF_2 is stable in both oxygen and hydrogen at temperatures as high as 760°C . Calculations for other materials and environments are done in a similar manner.

APPENDIX B

RECOMMENDED GRINDING PROCEDURE

1. Use diamond grinding only.
2. Use water as lubricant - use no oil.
3. Initial grinding depth should be 0.025 mm.
4. Final cuts should be 0.010 to 0.015 mm.

-Taking too deep a cut, i.e. 0.10 mm, will pluck softer phases (Ag and $\text{BaF}_2/\text{CaF}_2$) from surface.

-Taking too light a cut, i.e. less than 0.010 mm, will smear the metal-bonded chromium carbide. This will result in an "Orange Peel" type finish.

5. Ground surface should be matte, not glossy, and have a speckled appearance representing the three separate phases.

APPENDIX C

ERROR ANALYSIS

The experimental error for the data presented in this dissertation is analyzed in two ways. One is the precision with which the measurements are made; an external error analysis. This approach is used for the pin-on-disk tests. Another method, used for the foil bearing data, is to define the error in a statistical manner based upon similar data sets; an internal error analysis.

The External Error Analysis

The external error is based upon the precision with which physical measurements such as friction coefficient, rider wear factor and coating wear factor can be made (ref. 13).

The friction coefficient, μ , is defined as the friction force between two materials in relative motion divided by the normal force of the contact.

$$\mu = (\text{Friction Force})/(\text{Normal Force})$$

The external error associated with μ can, thus, arise from uncertainties in the magnitude of the applied load and inaccuracy in the measurement of the friction force.

The friction force is measured with a calibrated strain gage bridge. The uncertainty of this measurement system is approximately 3 percent. The load is applied by means of a dead weight system. Friction in the pulley system which transmit the applied load to the specimens and the load chamber feed-through system introduce an error of 5 percent. These uncertainty estimates are based upon calibration measurements of the test rig components. The overall error of the friction coefficient is estimated as the resultant of its parts:

$$\mu_{\text{external}} = ((3 \text{ percent})^2 + (5 \text{ percent})^2)^{1/2} = \pm 6 \text{ percent}$$

or for a typical friction coefficient of 0.3 the uncertainty is ± 0.02 .

The wear factor of the rider is based upon the following mathematical equation:

$$K_{\text{rider}} = \frac{(\text{volume of material worn})}{(\text{distance slid} \times \text{load})}$$

therefore the error of the K factor is dependent upon the inaccuracy in the measurement of the distance slid, load and wear volume. The following are typical estimates for the errors:

Error of wear volume = ± 11.5 percent

Error of distance slid = ± 2 percent

Error of load = ± 5 percent

$$K_{\text{rider external}} = ((11.5)^2 + (2)^2 + (5)^2)^{1/2} = \pm 12.7 \text{ percent}$$

The coating wear factor equation has the same general form as the rider wear factor equation, however the uncertainty of the wear volume is slightly smaller, 10 percent. Thus, the uncertainty of the coating wear factor is:

$$K_{\text{coating external}} = ((10)^2 + (2)^2 + (5)^2)^{1/2} = \pm 11.9 \text{ percent}$$

The Internal Error Analysis

The internal error estimate is used to determine the error in the data from the foil bearing rig. The uncertainties reported in the text represent one standard deviation of the data about an average. The sample population for the torque readings was fifty and the sample population for the foil and coating wear was 20. All of the specimens were fabricated at the same time with the same raw materials, therefore, specimen variations were minimized.

APPENDIX D

EXPLANATION OF WEAR FACTORS

The wear factor (K) used in this paper is a coefficient which relates the volume of material worn from a surface to the distance slid and the normal load at the contact. Mathematically, K is defined as:

$$K = \frac{1}{(S \times W)}$$

where

- W the normal load at the sliding contact in kilograms
- S the total distance slid in centimeters
- V the volume of material worn away in cubic centimeters

The physical interpretation of the numeric value of the K factor is as follows:

$K = 10^{-8} \text{ cm}^3/\text{cm-kg}$; high wear

$K = 10^{-9} \text{ to } 10^{-10} \text{ cm}^3/\text{cm-kg}$; moderate to low wear

$K = 10^{-11} \text{ cm}^3/\text{cm-kg}$; very low wear

Some authors prefer wear factor units of $\text{mm}^3/(\text{N-m})$. Conversion to these units can be made to a close approximation by multiplying our units by 10^4 .

TABLE I. - COMPOSITION OF THE THREE
MAJOR COATING COMPONENTS

Component	Composition, wt %	Particle size
Bonded chromium carbide		
Ni	28	-200 - 400 Mesh
Al	2	
Cr ₃ C ₂	58	
Co	12	
Silver metal		
Ag	100	-100 + 325
Prefused eutectic		
BaF ₂	62	-200 + 325
CaF ₂	38	

TABLE II. - TYPICAL PLASMA SPRAY PARAMETERS

Parameter	Material, value
Arc gas, 1.4 m ³ /hr	Argon
Powder carrier gas, 0.4 m ³ /hr	Argon
Coating powder flow rate, kg/hr	1
Amperage, A	450 to 475
Voltage, V	32
Gun to specimen distance, mm	~150

TABLE III. — NOMINAL COMPOSITION AND ROCKWELL HARDNESS OF CANDIDATE PISTON RINGS MATERIALS

Pin material code	Pin material	Element, wt %														Rockwell hardness
		Ni	Cr	Co	C	Fe	Al	Si	Ti	Mo	Mn	B	W	N	Cb	
Alloy A	Inconel X-750	70	16	1	0.1	7.5	1	—	2.5	—	1	—	—	—	—	R _C 40
Alloy B	XF818	18	18	—	.2	54.6	—	0.3	—	7.5	.15	0.7	—	0.12	0.4	R _C 18
Alloy C	Stellite 6B	2	30	59	1	1	—	.75	—	.75	1.25	—	4	—	—	R _C 42
Alloy D	Nitronic 60	8	18	.1	.1	61.8	—	4.0	—	—	.8	—	—	—	—	R _C 28

*Note: Compositions taken from manufacturer's data. Hardness values taken at room temperature.

TABLE IV. - SUMMARY OF BEARING STARTING AND STOPPING TORQUE FOR VARIOUS
COATING COMPOSITIONS

Coating I.D. number	Total wt % lubricant additives	T startup, N-mm	T stopping, N-mm	T startup, N-mm	T stopping, N-mm
		Room temperature		650 °C	
PS218	0	106.7±10.6	129.4±7.0	82.7±1.4	95.4±4.2
PS200	20	109.6±6.4	118.1±4.2	89.8±9.9	96.8±9.9
PS212	30	99.0±13.4	114.5±12.0	69.3±8.5	96.1±13.4
PS213	40	111.0±12.0	120.9±7.8	101.1±13.4	108.2±13.4

TABLE V. - SUMMARY OF FOIL WEAR FOR FOILS SLID AGAINST
VARIOUS JOURNAL COATINGS AFTER 9000 START/STOP CYCLES

Coating I.D. number	Percent reduction in foil thickness	Foil thickness wear, mm
PS218	55	0.056
PS200	25	.025
PS212	17.5	.018
PS213	22.5	.023

TABLE VI. - SUMMARY OF COATING WEAR FACTOR, K, FOR
VARIOUS JOURNAL COATINGS

Coating I.D. number	Total wt % added lubricants	K factor, in cc/cm-kg	K factor, in mm ³ /N-m
PS218	0	1.7×10^{-10}	1.7×10^{-6}
PS200	20	8.6×10^{-10}	8.8×10^{-6}
PS212	30	6.4×10^{-10}	6.5×10^{-6}
PS213	40	10.5×10^{-10}	10.7×10^{-6}

TABLE VII. - BEARING LOAD CAPACITY FOR VARIOUS JOURNAL
MATERIALS AND SURFACE FINISHES AT ROOM TEMPERATURE

Journal material	Surface finish, $\mu\text{m rms}$	Load capacity, kPa
Inconel 718	0.101±0.005	51
PS200 As ground	0.81±0.05	28
PS200 After run-in of 1000 start/stop cycles	0.152±0.010	41

TABLE VIII. - FRICTION AND WEAR TEST RESULTS
[Test conditions: 4.9-N load, 2.7-m/sec sliding velocity, Helium atmosphere.]

Test temperature, °C	Silver overlay thickness, NM	Friction coefficient	Pin wear factor		Coating wear factor	
			cm ³ /cm-kg	mm ³ /N-m	cm ³ /cm-kg	mm ³ /N-m
760	0	0.26	1.10x10 ⁻¹⁰	1.12x10 ⁻⁶	8.75x10 ⁻¹⁰	8.93x10 ⁻⁶
	25	.34	.21	.21	5.00	5.10
	50	.29	.84	.86	11.20	11.43
	75	.24	.87	.89	14.60	14.90
	100	.20	.42	.43	7.01	7.15
	125	.23	.66	.67	9.30	9.49
	150	.31	.48	.49	14.00	14.29
	200	.33	.98	1.00	22.00	22.45
	350	.40	.73	.74	20.00	20.41
350	0	0.19	0.40	0.41	2.80	2.86
	25	.28	.69	.70	1.20	1.22
	50	.24	.51	.52	4.80	4.90
	75	.19	.23	.23	3.60	3.67
	100	.16	.16	.16	2.96	2.96
	125	.19	.33	.34	1.02	1.02
	150	.19	.40	.41	4.08	4.08
	200	.22	.17	.17	4.08	4.08
	350	.21	.56	.57	3.37	3.37
25	0	0.19	0.18	0.18	1.70	1.73
	25	.34	.32	.33	3.10	3.16
	50	.25	.49	.50	5.60	5.71
	75	.22	.29	.30	4.40	4.49
	100	.17	.08	.08	4.10	4.18
	125	.20	.08	.08	1.65	1.68
	150	.21	.20	.20	4.70	4.80
	200	.16	.06	.06	1.00	1.02
	350	.20	.13	.03	1.70	1.73

TABLE IX. - WEAR FACTOR RATIO

Test temperature, °C	Silver film thickness, nm	$K_{pin}/K_{coating}$ ratio
760	0	0.120
	25	.042
	50	.075
	75	.059
	100	.059
	125	.070
	150	.034
	200	.044
	350	.036
350	0	0.142
	25	.058
	50	.106
	75	.063
	100	.055
	125	.330
	150	.097
	200	.042
	350	.169
25	0	0.105
	25	.106
	50	.087
	75	.075
	100	.019
	125	.050
	150	.042
	200	.062
	350	.076

TABLE X. - SPUTTERING PARAMETERS USED TO APPLY SOLID LUBRICANT FILMS TO THE SPECIMENS

Coating material	Thickness, nm	Sputtering time, min	Power, kW	Argon flowrate, cc/min	Chamber pressure, mTorr
CaF ₂	50	17	1	12	10
Ag	100	0.5	0.5	12	10
Au	150	10.0	0.05	≈10	50
Rh	150	12.5	0.20	≈10	10
Pd	50	5.0	0.20	≈10	10

TABLE XI. - FRICTION AND WEAR DATA SUMMARY FROM FABRIC TRIBOTEST

[Note: Extent of fiber breakage: Severe; more than 100 broken fibers in one bundle. Moderate; more than 40 but less than 100 broken fibers in one bundle, Mild; less than 30 to 40 broken fibers in one bundle.]

Fabric coating or lubricant treatment	Disk material	Friction coefficient		Fabric fiber breakage
		25 °C	850 °C	
none	Inconel X750	0.60±0.03	1.30±0.05	Moderate
none	Copper	0.30±0.02	0.50±0.03	None
1000 nm Ag	Inconel X750	0.30±0.02	-----	None
500 nm CaF ₂	Inconel X750	-----	0.60±0.03	None
1000 nm Ag + 500 nm CaF ₂	Inconel X750	0.30±0.02	0.60±0.03	None
150 nm Au	Inconel X750	0.30±0.02	0.60±0.03	None
≈0.1 mm B	Inconel X750	0.05±0.03	1.30±0.05	Moderate

TABLE XII. - SUMMARY OF Ti₃Al-Nb SLIDING AGAINST CERAMIC FABRIC

[Note: Extent of fiber breakage: Severe; more than 100 broken fibers in one bundle. Moderate; more than 40 but less than 100 broken fibers in one bundle. Mild; less than 30 to 40 broken fibers in one bundle.]

Fabric coating or lubricant treatment	Disk coating or lubricant treatment	Final friction coefficient		Fiber breakage	Comments
		25 °C	700 °C		
None	None	1.3±0.2	1.3±0.2	Severe	No material transfer
150 nm AU film (sputtered)	None	1.0±0.2	1.3±0.1	Severe	No Au transfer to disk
None	150 nm Au film (sputtered)	1.8±0.1	1.4±0.2	Moderate	Poor Au adhesion to disk
None	150 nm Au film (ion plated)	0.20±0.05 (initial value)	Test ter- minated at 450 °C	Severe	Fabric failed. Tested only to 450 °C
None	150 nm AU film over 150 nm Rh film (sputtered)	0.6±0.1	1.0±0.1	Mild	Smooth final surface

ORIGINAL PAGE
BLACK AND WHITE PHOTOGRAPH

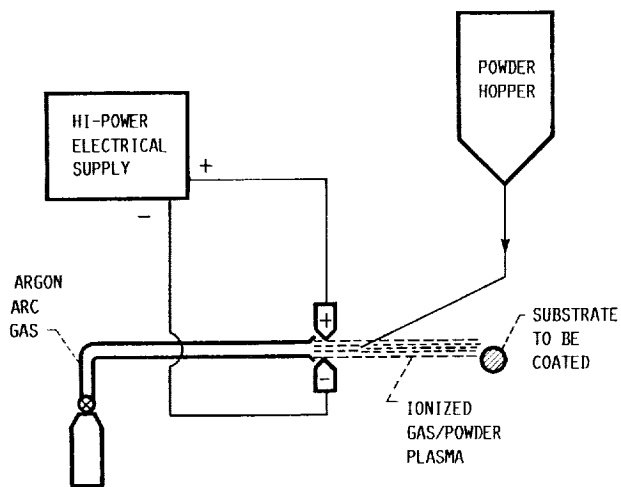


FIGURE 1. - SCHEMATIC OF PLASMA-SPRAY PROCESS.



FIGURE 2. - PLASMA-SPRAYED GAS BEARING JOURNAL.



FIGURE 3. - DIAMOND GROUND GAS BEARING JOURNAL.

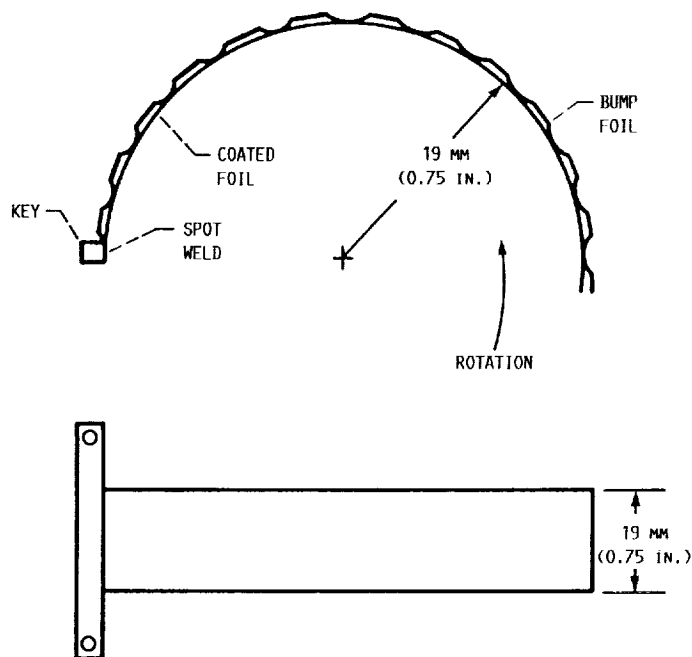


FIGURE 4A. - COMPLIANT FOIL GAS BEARING ASSEMBLY.

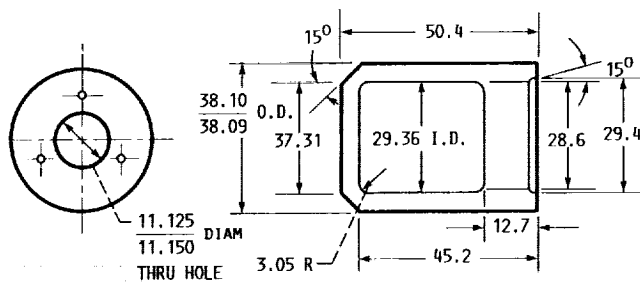


FIGURE 4B. - JOURNAL FOR COMPLIANT GAS BEARING. MATERIAL, INCONEL 718. DIMENSIONS IN MILLIMETERS.

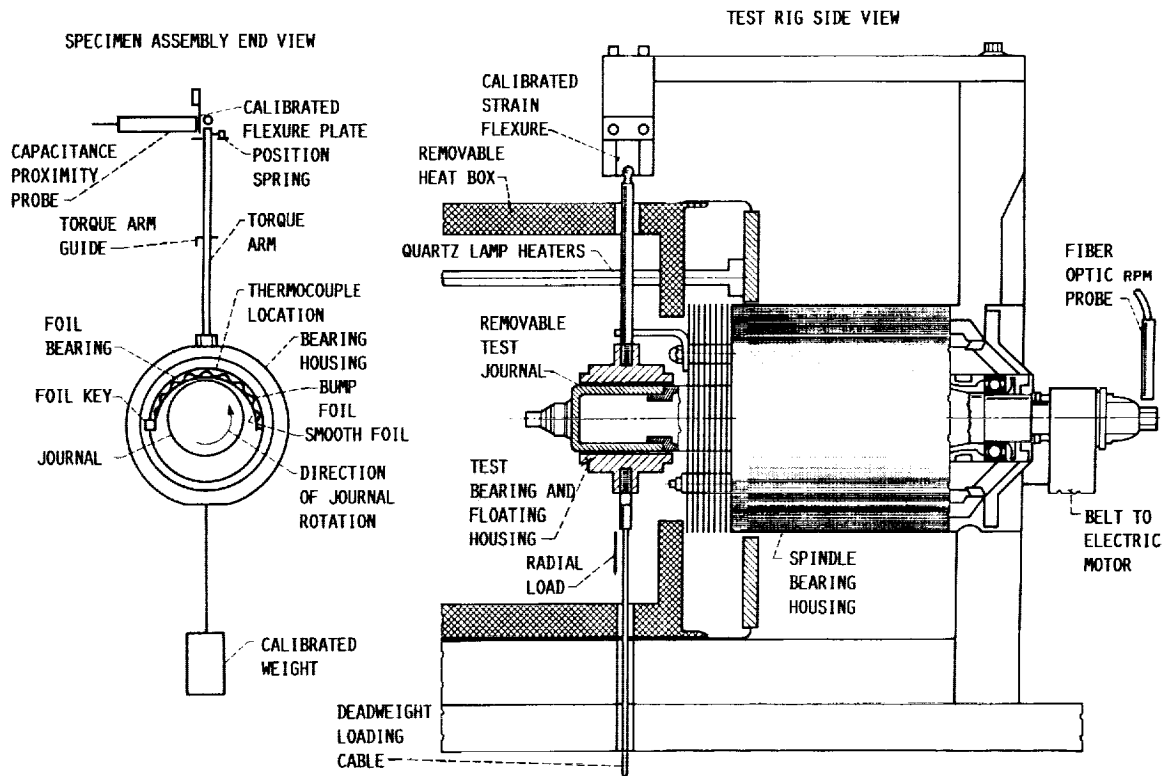


FIGURE 5. - FOILS JOURNAL BEARING MATERIALS TEST RIG AND END VIEW OF BEARING AND JOURNAL DURING TESTING.

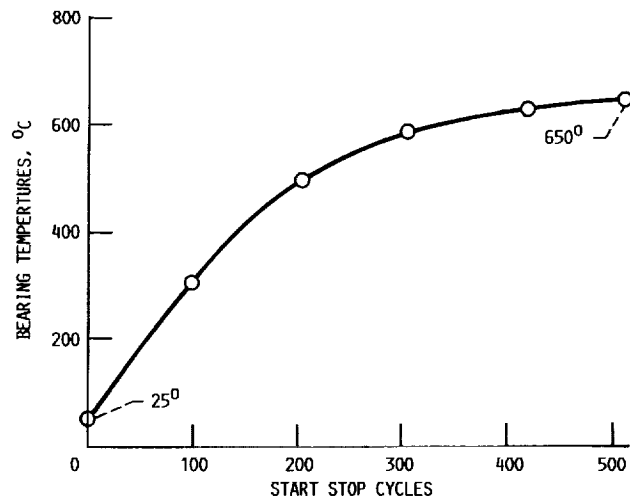


FIGURE 6. - TEST TEMPERATURE DURING 500 START/STOP CYCLES HEATING FROM 25 °C TO 650 °C.

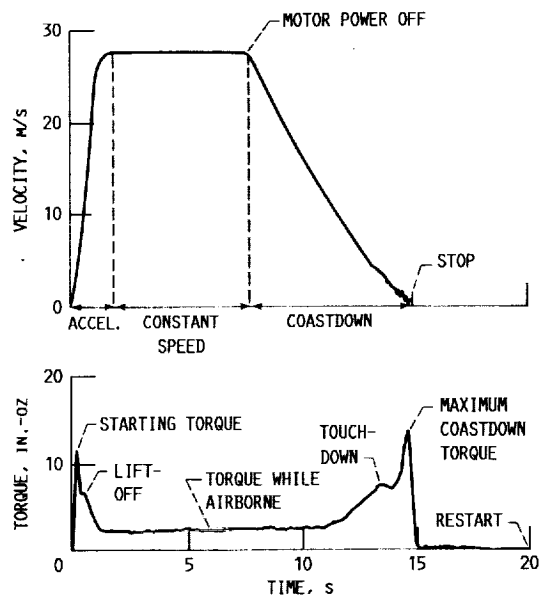


FIGURE 7. - TYPICAL TORQUE PROFILE OF A FOIL BEARING DURING A SINGLE START/STOP CYCLE.

ORIGINAL PAGE
BLACK AND WHITE PHOTOGRAPH

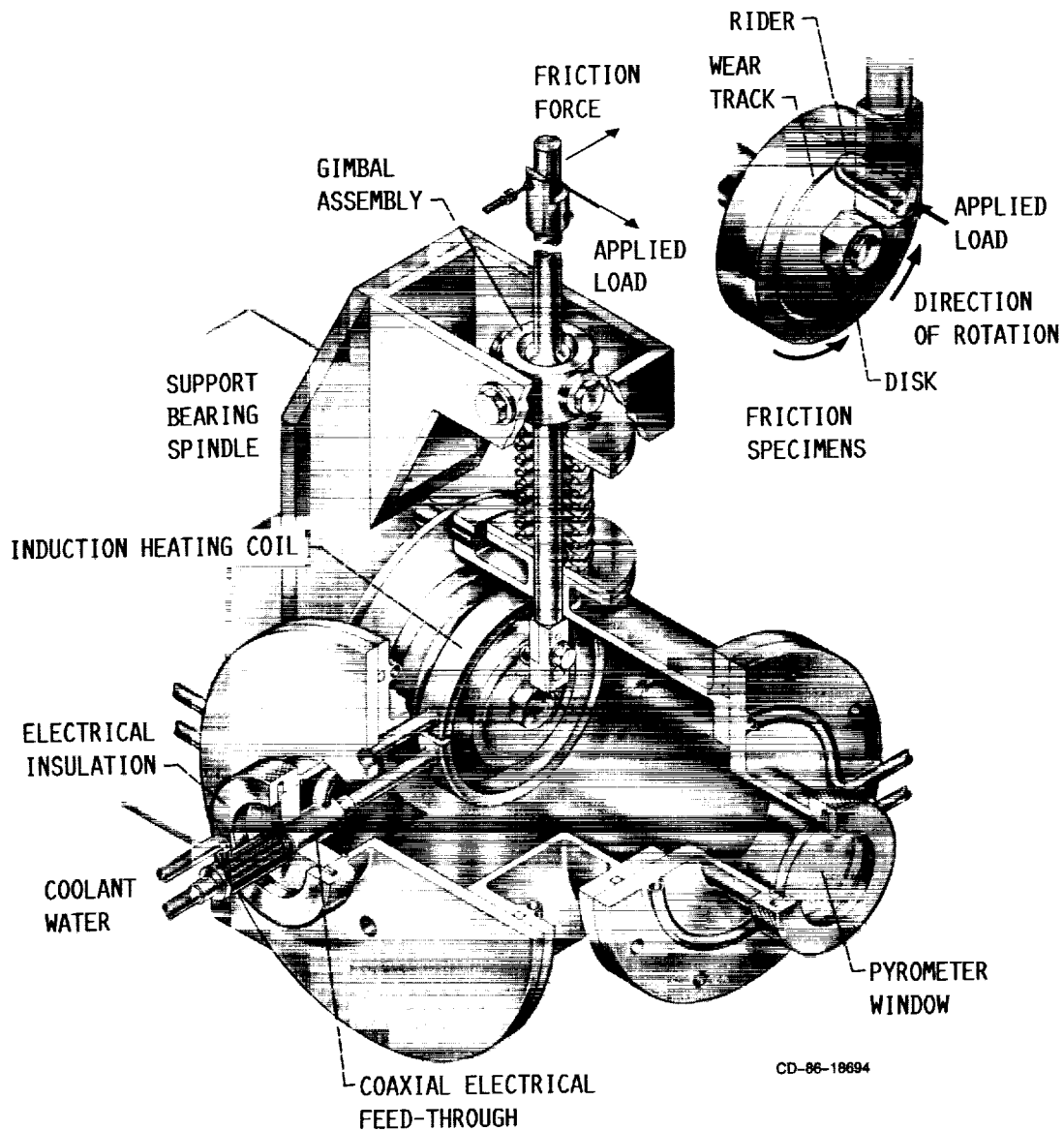


FIGURE 8. - HIGH TEMPERATURE PIN-ON-DISK RIG.

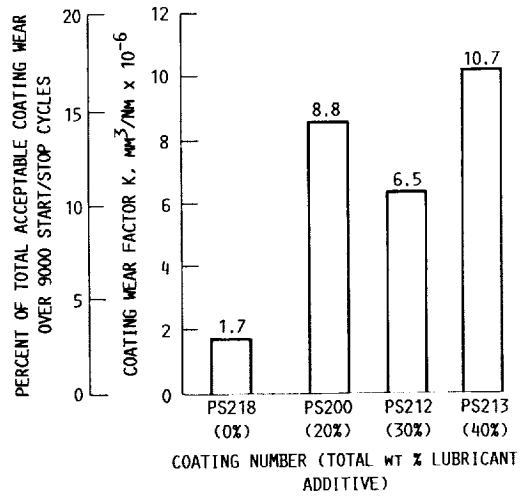


FIGURE 9. - JOURNAL COATING WEAR FACTOR, K, FOR THE VARIOUS COATING COMPOSITIONS TESTED.

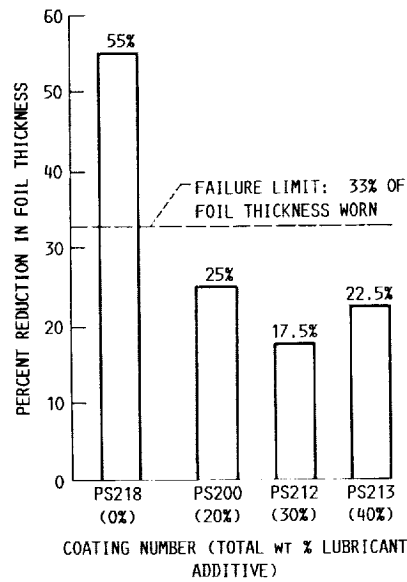


FIGURE 10. - FOIL WEAR VERSUS JOURNAL COATING COMPOSITION: TEST CONDITIONS: 9000 START/STOP CYCLES, 14 KPA LOAD.

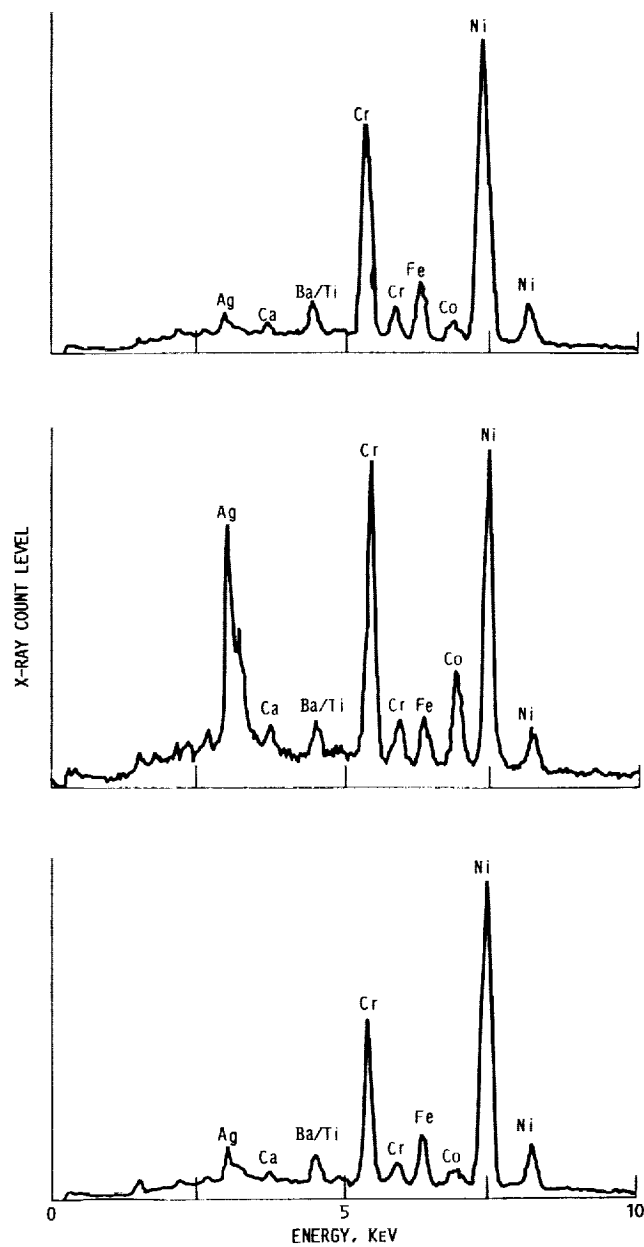


FIGURE 11. - EDS X-RAY SPECTRA FOR FOIL SURFACE AFTER SLIDING AGAINST MODIFIED COATINGS WITH LUBRICANT ADDITIVES.

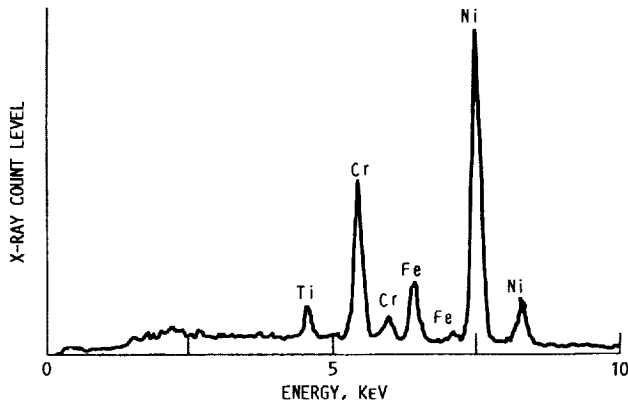


FIGURE 12. - EDS X-RAY SPECTRUM OF FOIL SURFACE AFTER SLIDING AGAINST UNMODIFIED COATING (PS218) WITH NO LUBRICANT ADDITIVES.

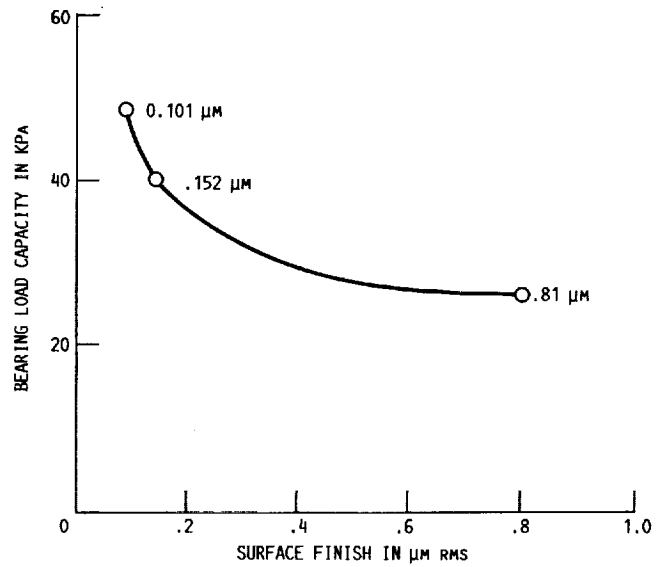


FIGURE 13. - BEARING LOAD CAPACITY VERSUS JOURNAL SURFACE FINISH. SURFACE VELOCITY 26.7 m/s, ROOM TEMPERATURE.

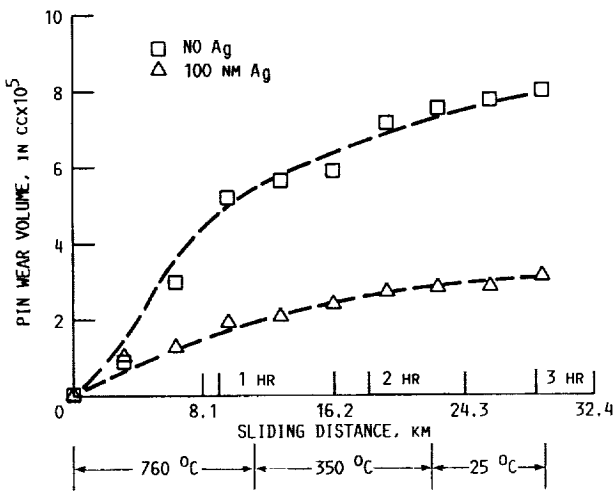


FIGURE 14. - PIN WEAR VOLUME VERSUS SLIDING DISTANCE. TEST CONDITIONS: 4.9 N LOAD, 2.7 m/s SLIDING VELOCITY, HELIUM ATMOSPHERE.

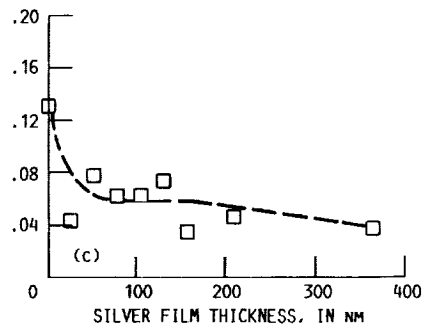
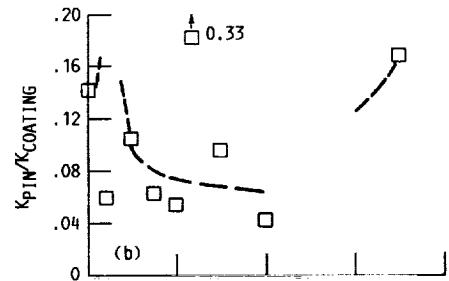
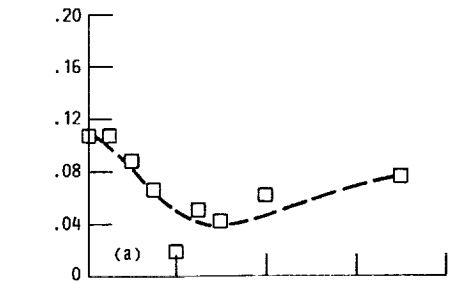


FIGURE 15. - WEAR FACTOR RATIO VERSUS SILVER FILM OVERLAY THICKNESS.

ORIGINAL PAGE
BLACK AND WHITE PHOTOGRAPH



FIGURE 16. - ARTIST'S CONCEPTION OF HYPERSONIC FLIGHT VEHICLE (NASP).

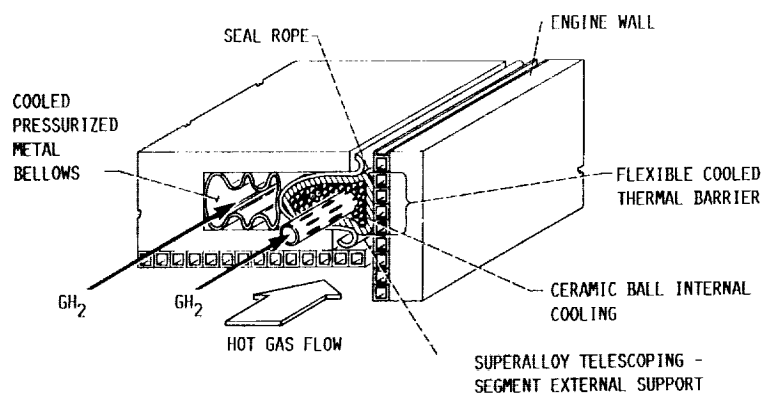


FIGURE 17. - CROSS SECTION OF PROPOSED ENGINE SEAL.

ORIGINAL PAGE
BLACK AND WHITE PHOTOGRAPH

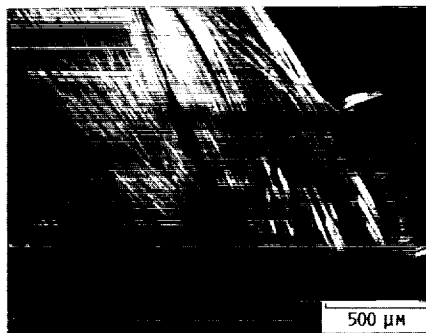


FIGURE 18. - VIRGIN FABRIC BUNDLES.

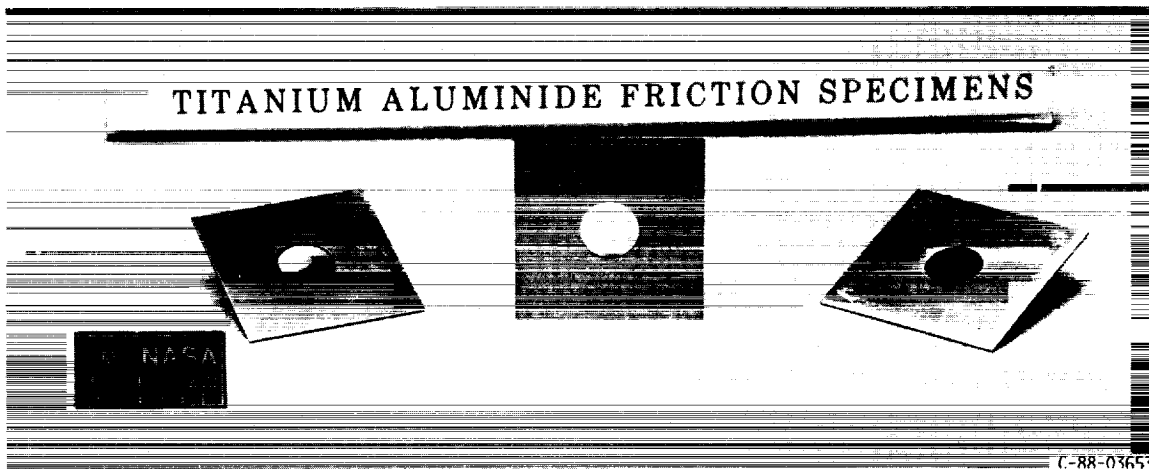


FIGURE 19. - Ti_3Al-Nb INTERMETALLIC TEST DISKS.

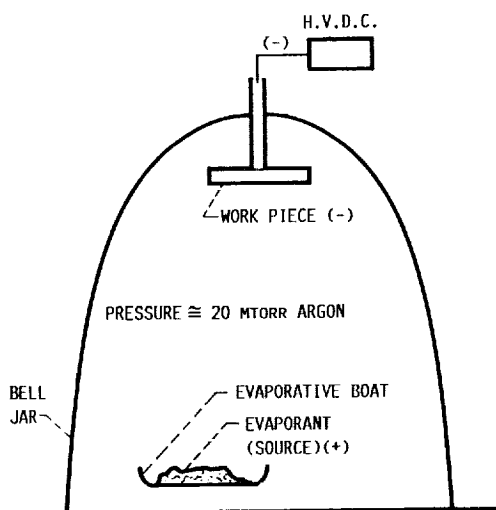


FIGURE 20. - ION PLATING.

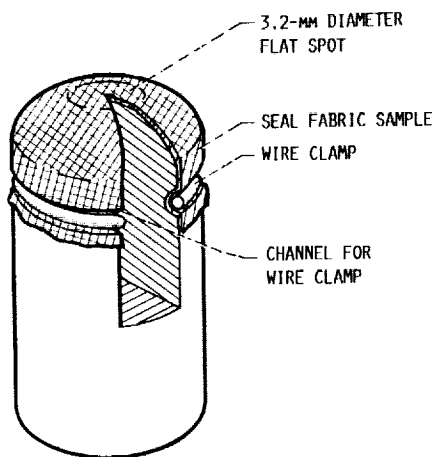


FIGURE 21. - PIN TEST SPECIMEN.

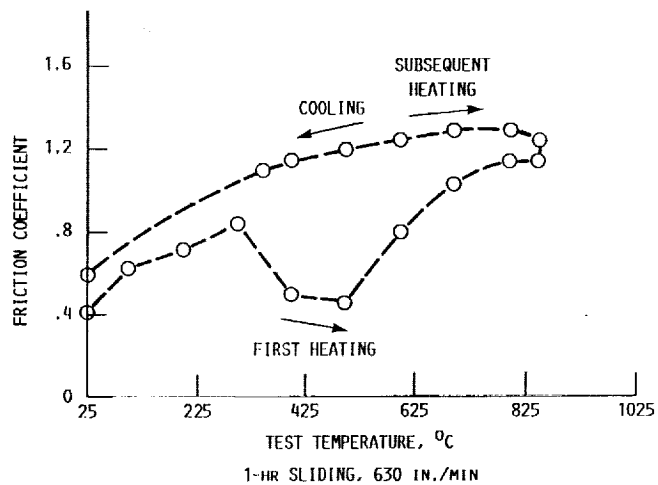


FIGURE 22. - FRICTION COEFFICIENT FOR FABRIC SLIDING AGAINST INCONEL WITH NO LUBRICANT COATINGS.

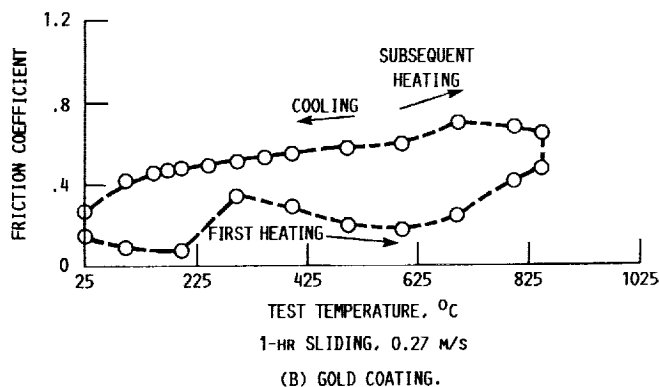
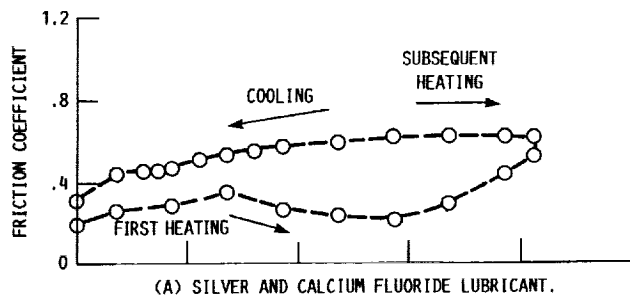


FIGURE 23. - FRICTION COEFFICIENT FOR FABRIC SLIDING AGAINST INCONEL TEST DISK.

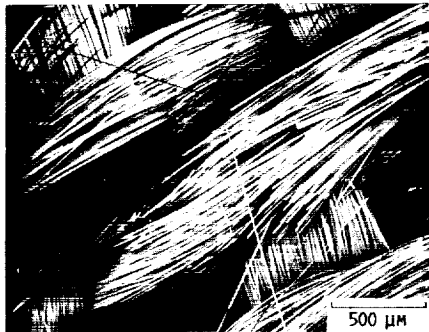


FIGURE 24. - FABRIC FRACTURE AFTER SLIDING AGAINST INCONEL DISK. NO LUBRICANTS APPLIED.

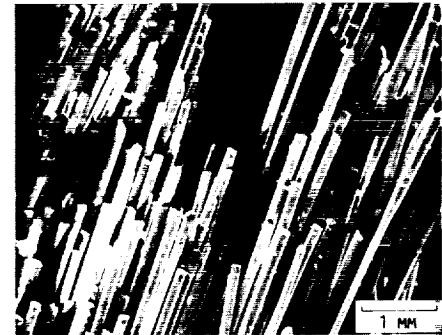


FIGURE 25. - FRACTURED CERAMIC FIBERS.

ORIGINAL PAGE
BLACK AND WHITE PHOTOGRAPH

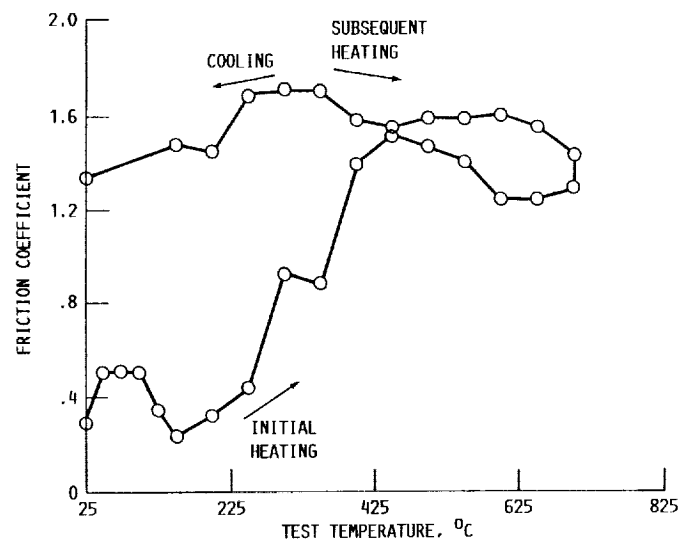


FIGURE 26. - FRICTION COEFFICIENT FOR FABRIC SLIDING AGAINST Ti_3Al-Nb INTERMETALLIC DISK. AIR ATMOSPHERE, 0.27 KG LOAD, 0.27 M/S SLIDING VELOCITY.

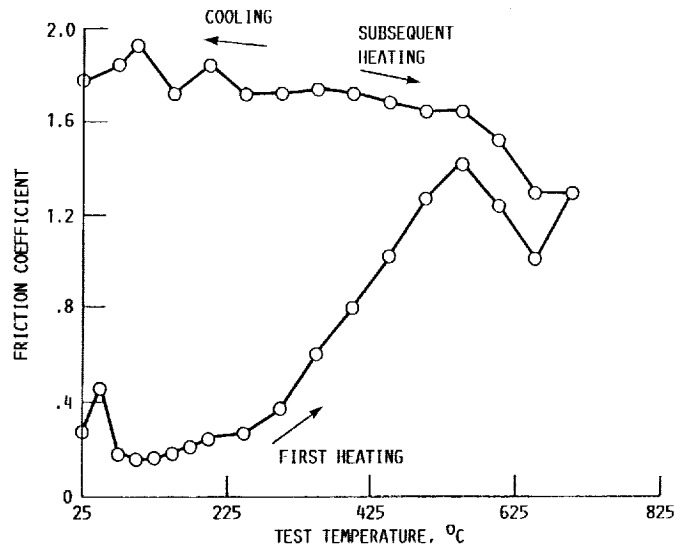


FIGURE 27. - FRICTION COEFFICIENT FOR THE FABRIC COATED WITH 150 NM GOLD WHEN SLIDING AGAINST THE Ti_3Al-Nb INTERMETALLIC DISK. AIR ATMOSPHERE, 0.27 KG LOAD, 0.27 M/S SLIDING VELOCITY.

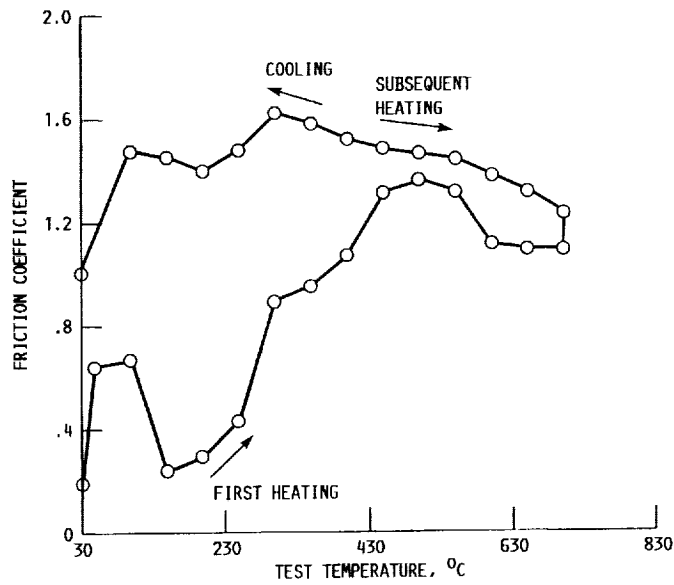


FIGURE 28. - FRICTION COEFFICIENT FOR FABRIC SLIDING AGAINST A GOLD COATED Ti_3Al-Nb DISK. AIR ATMOSPHERE, 0.27 KG LOAD, 0.27 M/S SLIDING VELOCITY.

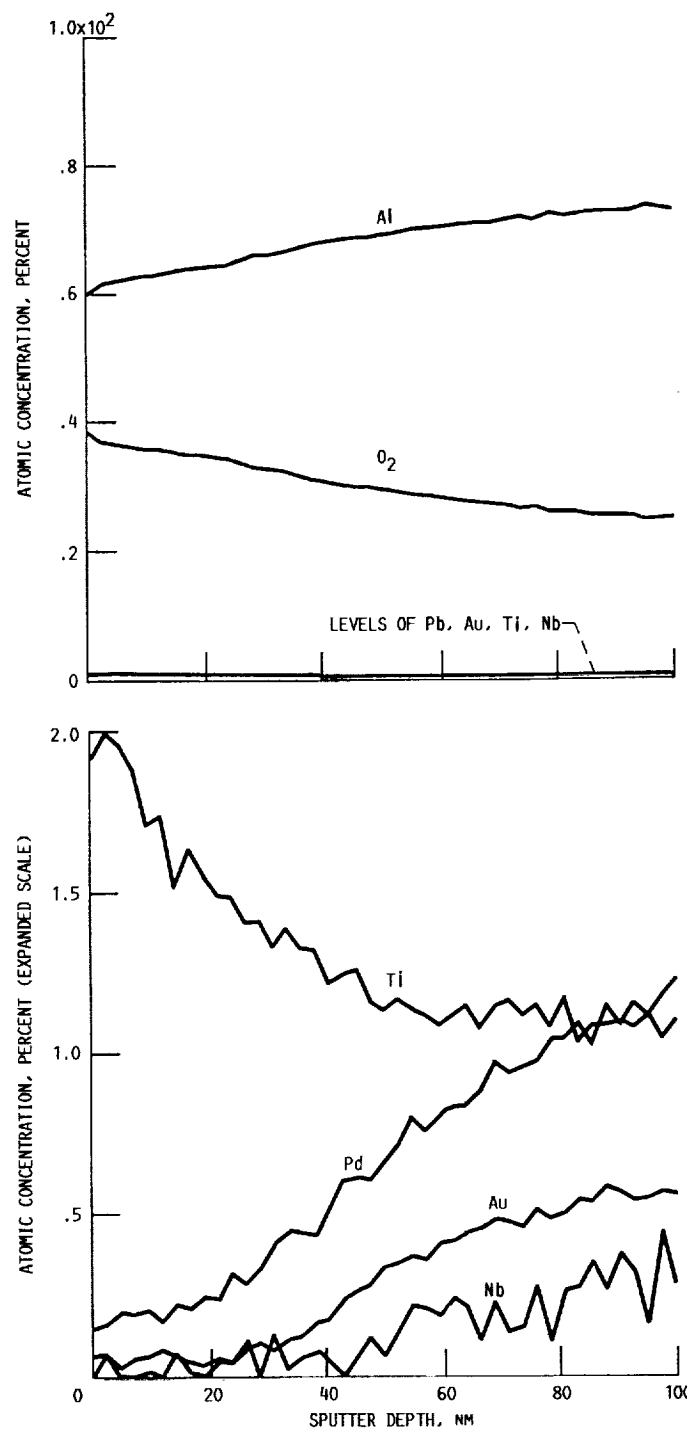


FIGURE 29. - XPS DEPTH PROFILE RESULTS OF HEAT TREATED INTER-METALLIC WHICH WAS COATED WITH 50 NM PALADIUM AND 100 NM OF GOLD.

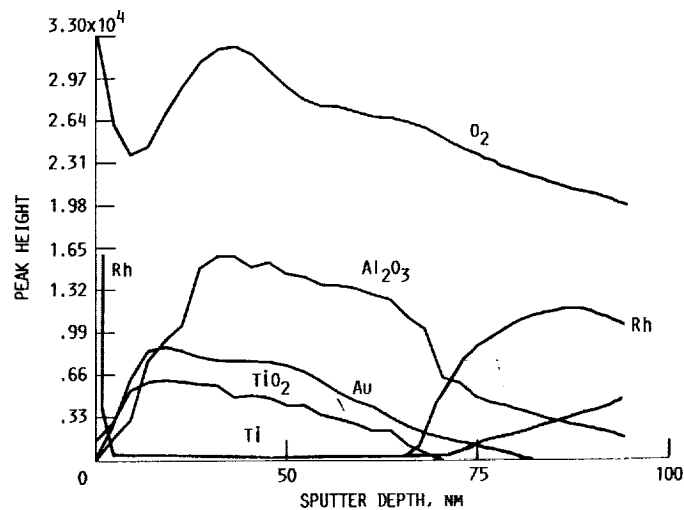


FIGURE 30. - XPS DEPTH PROFILE OF HEAT TREATED INTERMETALLIC SPECIMEN COATED WITH 50 NM RHODIUM AND 100 NM OF GOLD.

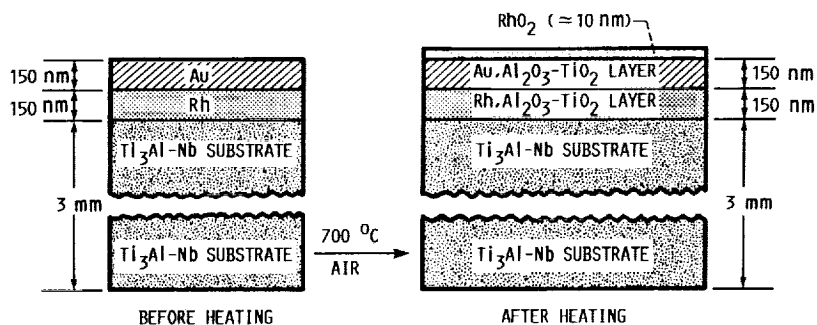


FIGURE 31. - MODEL OF INTERMETALLIC FILM LAYER COMPOSITION BEFORE AND AFTER HEAT TREATMENT IN AIR AT 700 °C.

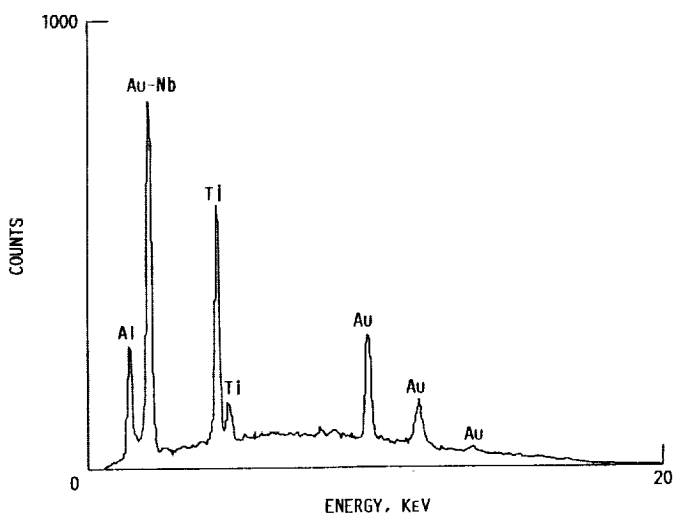


FIGURE 32. - EDS X-RAY SPECTRUM OF Ti_3Al-Nb DISK ION PLATED WITH GOLD AND SLID AGAINST FABRIC AT 700 °C. NO POST TEST SURFACE PREPARATION MADE PRIOR TO ANALYSIS.

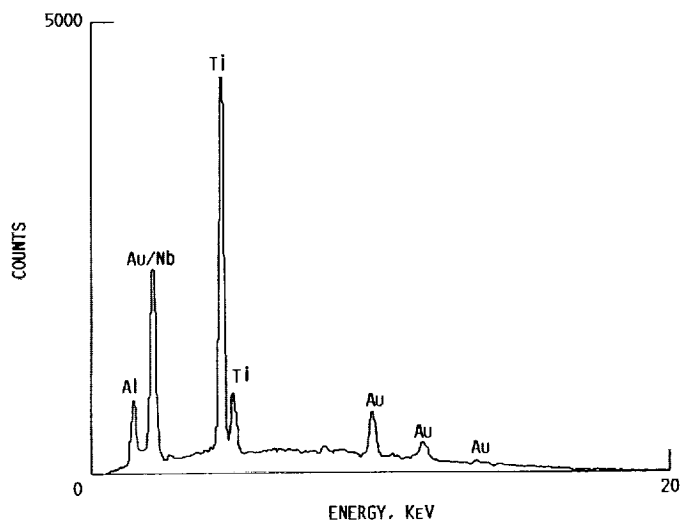


FIGURE 33. - EDS X-RAY SPECTRUM OF Ti_3Al-Nb DISK ION PLATED WITH GOLD AFTER SLIDING AGAINST FABRIC AT 700 °C. SURFACE SCRAPPED PRIOR TO ANALYSIS.



National Aeronautics and
Space Administration

Report Documentation Page

1. Report No. NASA TM-102476 DOE/NASA/50162-3		2. Government Accession No.		3. Recipient's Catalog No.	
4. Title and Subtitle The Experimental Evaluation and Application of High-Temperature Solid Lubricants				5. Report Date January 1990	
				6. Performing Organization Code	
7. Author(s) Christopher DellaCorte				8. Performing Organization Report No. E-5263	
				10. Work Unit No. 505-63-1A	
9. Performing Organization Name and Address National Aeronautics and Space Administration Lewis Research Center Cleveland, Ohio 44135-3191				11. Contract or Grant No.	
				13. Type of Report and Period Covered Technical Memorandum	
12. Sponsoring Agency Name and Address U.S. Department of Energy Office of Vehicle and Engine R&D Washington, D.C. 20545				14. Sponsoring Agency Code	
15. Supplementary Notes Final Report. Prepared under Interagency Agreement DE-AI01-85CE50162. This report was submitted as a dissertation in partial fulfillment of the requirements for the degree Doctor of Philosophy to Case Western Reserve University, Cleveland, Ohio in May 1989.					
16. Abstract This dissertation describes a research program meant to develop an understanding of high-temperature solid lubrication and experimental techniques through the development of a composite lubricant coating system. The knowledge gained through this research was then applied to a specific engineering challenge, the tribology of a sliding seal for hypersonic flight vehicles. The solid lubricant coating is a chromium carbide based composite combined with silver, which acts as a low temperature lubricant, and barium fluoride/calcium fluoride eutectic, which acts as a high temperature lubricant. This composite coating provides good wear resistance and low friction for sliding contacts from room temperature to over 900 °C in reducing or oxidative environments. The specific research on this coating included a composition screening using a foil gas bearing test rig and the use of thin silver films to reduce initial wear using a pin-on-disk test rig. The chemical stability of the materials used was also addressed. This research indicated that soft metallic films and materials which become soft at elevated temperatures are potentially good lubricants. The general results from the experiments with the model solid lubricant coating were then applied to a sliding seal design concept. This seal design requires that a braided ceramic fabric slide against a variety of metal counterface materials at temperatures from 25 to 850 °C in an oxidative environment. A pin-on-disk tribometer was used to evaluate the tribological properties of these materials and to develop lubrication techniques. The results of this work indicate that these seal materials must be lubricated to prevent wear and reduce friction. Thin films of silver, gold and calcium fluoride provided lubrication to the sliding materials. The data obtained and the lubrication techniques developed in this study provide important information to designers of sliding seals.					
17. Key Words (Suggested by Author(s)) Lubrication Solid lubricant High-temperatures Seals			18. Distribution Statement Unclassified - Unlimited Subject Category 27 DOE Category UC-96		
19. Security Classif. (of this report) Unclassified		20. Security Classif. (of this page) Unclassified		21. No. of pages 58	
				22. Price* A03	

